Elastic Sensing Skin for Monitoring of Concrete Structures

by

Emmanuel Abiodun Ogunniyi

Bachelor of Engineering
Federal University of Technology, Akure 2018

Submitted in Partial Fulfillment of the Requirements

for the Degree of Masters of Science in

Mechanical Engineering

College of Engineering and Computing

University of South Carolina

2023

Accepted by:

Austin Downey, Director of Thesis

Subramani Sockalingam, Reader

Ann Vail, Dean of the Graduate School

Dedication

To those who inspire, empower, and transform the implausible into reality for me, I dedicate this thesis to you.

To my Family: You stand as the foundational pillars of my strength, guiding beacons during my bleakest moments, and the unwavering wellspring of my determination. It's your boundless love and support that has propelled me through this academic odyssey, shining a light towards my aspirations.

To my Friends: Throughout this remarkable journey, you have been my cherished companions, infusing moments of labor with joy and offering steadfast support when burdens grew heavy. With you, I discovered the harmony between diligence and delight, and for this, my gratitude knows no bounds.

To my Advisor, Dr. Austin R.J. Downey: Your sagacious guidance, invaluable mentorship, and deep-rooted knowledge have acted as my compass in the vast sea of research. Your unwavering belief in my potential has elevated my ambitions and spurred me onwards. Your support has been an integral part of this journey.

This thesis embodies the tenacious spirit of exploration and an insatiable quest for understanding.

With heartfelt gratitude and a profound sense of purpose,

Emmanuel Abiodun Ogunniyi

Acknowledgments

The authors gratefully acknowledge the financial support of the Departments of Transportation of Iowa, Kansas, South Carolina, and North Carolina, through the Transportation Pooled Fund Study TPF-5(449).

Abstract

Soft elastomeric capacitors (SECs) are emerging as potential low-cost solutions for monitoring cracks and strains in concrete infrastructure, a crucial aspect of structural health monitoring. Effective long-term monitoring of civil infrastructure can reduce the risk of structural failures and potentially reduce the cost and frequency of inspections. However, deploying structural health monitoring (SHM) technologies for bridge monitoring is expensive, especially long-term, due to the density of sensors required to detect, localize, and quantify cracks. Previous research on soft elastomeric capacitors (SEC) has shown their viability for low-cost monitoring of cracks in transportation infrastructure. However, when deployed on concrete for strain monitoring, a structure/sensor capacitive coupling exists that may cause a significant amplification in the signal collected from the SEC sensor. This work provides a detailed experimental study of electrically isolating capacitive sensing skins for concrete structures to reduce the electrically grounded sensor's structure/sensor capacitive coupling. The study illustrates that using rubber isolators effectively decreases the capacitive coupling between concrete, which inherently has capacitive properties and sensors such as the SEC that utilize capacitance measurements. By investigating rubber isolators, we found that isolation thicknesses between 0.30mm and 0.64mm significantly reduced this capacitive interference, with approximately 0.40mm displaying the optimal response. Secondly, in addressing the challenge of electrical coupling, robust isolation of the SECs from the concrete is done by extending the styrene-block-ethylene-co-butylene-block-styrene matrix of the SECs to include a decoupling layer between the electrode and the concrete instead of a rubber isolator. Experimental results showed

this modification lowered the nominal capacitance of the SEC, making them viable for concrete strain monitoring. Comparisons were drawn with conventional resistive strain gauges, emphasizing the modified SECs' potential. Lastly, the adhesion of SECs onto surfaces is vital for their efficacy. Two adhesion methods were investigated: direct painting with carbon black (CB) and epoxy bonding. Although cost-effective and quick, CB posed durability concerns, whereas epoxy bonding offered high adhesion strength, albeit with a more complex application process. Overall, this comprehensive study enlightens the challenges and solutions of deploying SECs on concrete surfaces. It offers insights for their improved performance and broader applicability in civil infrastructure monitoring.

Table of Contents

List of Tables

List of Figures

Chapter 1

Introduction

Bridges, concrete structures, and metallic surfaces are vital elements in civil engineering. Ensuring these structures' safety, longevity, and optimal performance is paramount. Structural health monitoring (SHM) has emerged as a crucial tool to address these concerns, providing insights into the real-time health and performance of structures, ensuring public safety, and optimizing maintenance strategies [6, 7, 8, 9, 10, 11, 12]. However, the effectiveness of SHM largely depends on the sensors' capability to capture and report accurate data on the behavior and performance of structures. Figure 1.1(a) and (b) shows cracks in bridge that could result to complete failure of the bridge if not monitored and repaired. Early monitoring of structural behavior can prevent expensive maintenance. Sample traditional sensors such resistive strain gauges, Fiber Bragg gratings, linear variable differential transformers shown in Figure 1.1(c), (d), and (e) are used for monitoring of bridges, however, they are required in large number to accurately capture enough data to describe the structure which could be expensive.

Among the various sensors available, Soft Elastomeric Capacitors (SECs) have gained significant attention due to their flexibility, adaptability, and the ability to measure strain, pressure, and deformation [13, 14, 15]. Their applications span from structural health monitoring in bridges [16] to wearable electronics and healthcare [17, 18]. Notably, their potential in continuously monitoring large areas, like the surfaces of bridges and concrete structures, stands out [11, 19]. The SHM sector's evolution has seen the development of 'smart bridges', incorporating sensors directly

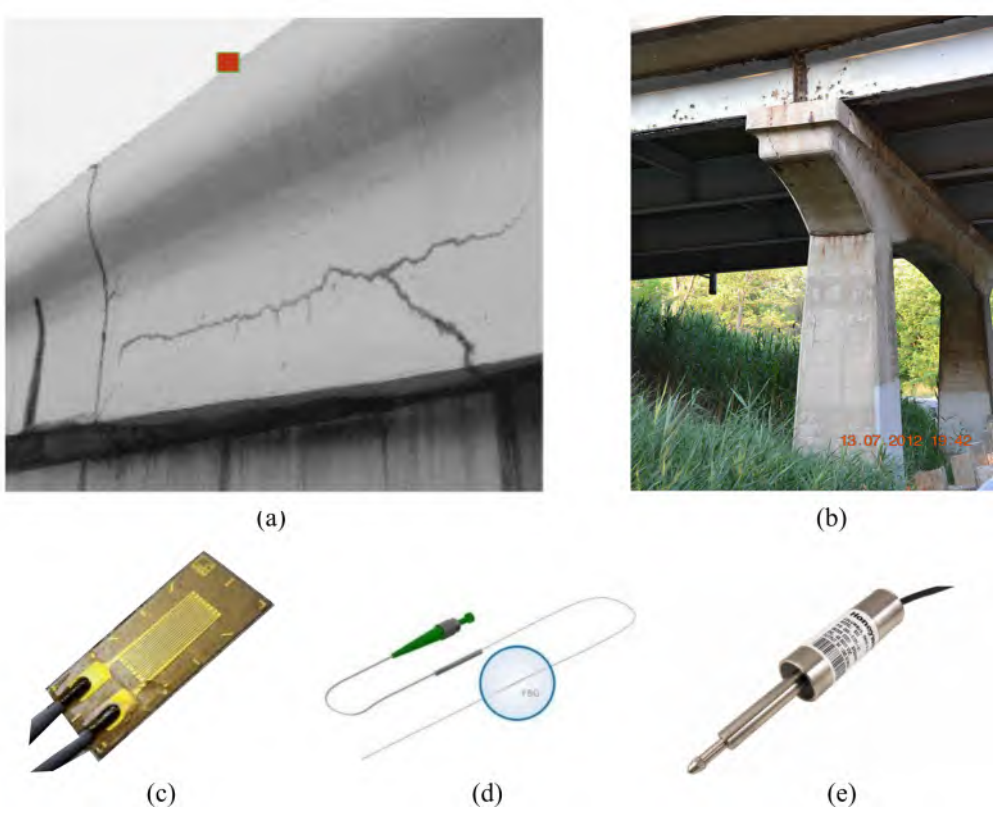

Figure 1.1 Crack formation on bridges which could potentially lead to structural failure, as shown in (a) long cracks on bridge [1] and (b) bridge showing a single crack on it [2], alongside traditional SHM sensors like (c) resistive strain gauge [3]; (d) Fiber Bragg gratings [4]; and (e) linear variable differential transformers [5].

into the construction process to provide real-time health insights [20]. Nevertheless, a few challenges remain, such as ensuring the precision of these sensors against varying environmental conditions and optimizing their adhesion to diverse surfaces for long-term monitoring.

SECs' effective use in concrete structures has been hampered by the inherent capacitive nature of concrete, leading to capacitive coupling and subsequent overestimation of strain data [21, 22]. Recent research efforts have suggested using rubber as an isolation material between the SEC and concrete to address this issue. Still, the deployment remains cumbersome [23]. Another avenue explored is the inclusion of an extended polymer matrix of styrene-block-ethylene-co-butylene-block-styrene (SEBS) in the SEC design, which acts as an integrated isolation layer [24]. This modification

promises to streamline the deployment process without compromising sensitivity.

Furthermore, the mode of adhering SECs to the monitored surface, whether concrete or metal, is equally crucial. Traditional methods like off-the-shelf epoxy might not provide the necessary robustness or longevity [25]. Hence, this research also embarks on a comprehensive study comparing two distinct adhesion methods for SECs: direct painting and epoxy bonding. This study aims to provide a holistic understanding of the best practices for deploying SECs on concrete and metallic surfaces by examining the strength, conductivity, and overall sensor functionality.

This work's primary objective is to optimize the use of SECs for SHM by addressing the challenges in deploying them on concrete structures and ensuring robust and reliable adhesion. The broader implications of this research will significantly influence the domains of civil engineering, healthcare, and wearable electronics, ensuring safer and more sustainable environments.

In the following sections, we delve deeper into the background of SECs, their recent advancements, the challenges faced, the methodology employed to compare adhesion techniques, and the consequential findings that promise to shape the future of structural health monitoring.

1.1 Proposal for Optimization and Application of Soft Elastomeric Capacitors in Structural Health Monitoring

1.1.1 Background:

Structural health monitoring (SHM) plays a pivotal role in ensuring the longevity and safety of various civil structures, especially bridges. A key challenge in the SHM domain has been the deployment of sensors across vast areas and diverse materials like steel and concrete. While current SHM technologies, such as strain gauge, corrosion sensors, and fiber-optic sensors, offer substantial insights, their precision can be limited due to external environmental factors. Among emerging solutions, Soft

Elastomeric Capacitors (SECs) have shown considerable promise for fatigue crack monitoring, strain detection, and other large-area monitoring applications. However, the adhesion of SECs onto substrates like concrete and metal remains a challenge, with potential issues such as capacitive coupling and delamination affecting the sensor's efficiency and lifespan.

1.1.2 Objective:

The primary aim of this research is to optimize SECs on concrete and metal surfaces to enhance their performance and reliability for SHM applications. The study will specifically focus on the following as shown in Figure 1.2:

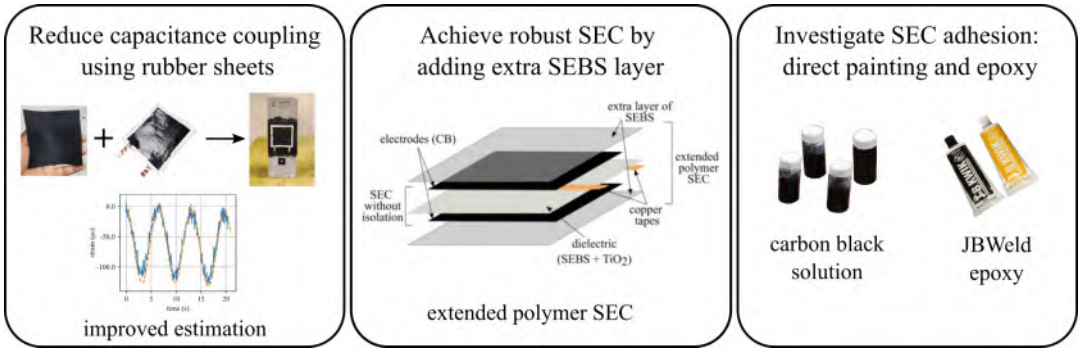

Figure 1.2 SEC-concrete deployment optimization process.

i. Reducing capacitance coupling between the SEC and concrete using rubber plate.

ii. Evaluating the effectiveness of an extended polymer matrix on the SEC.

iii. Investigate two distinct methods for adhering SECs: direct painting and epoxy bonding.

1.1.3 Methodology:

SECs Design Modification:

i. An extended polymer matrix of styrene-block-ethylene-co-butylene-block-styrene (SEBS) will be integrated into the SEC design. This matrix is expected to act as an isolation layer, minimizing capacitance coupling.

ii. The SEC design will incorporate corrugation, SEBS addition, and other innovations to ensure robust performance.

Adhesion Techniques:

i. Direct Painting: SECs will be directly painted onto prepared surfaces of concrete and metal. The longevity, stability, and performance of these SECs under diverse conditions will be assessed.

ii. Epoxy Bonding: Using specialized adhesives, SECs will be bonded onto the substrates. This method will be evaluated for its adhesion strength and robustness.

Experimental Setup:

i. SECs will be deployed across bridge mock-ups and subjected to real-world conditions that mimic wind, humidity, temperature variations, and strain changes.

ii. Commercially available resistive strain gauges and digital image correlation results will be used as benchmark data.

Data Analysis:

i. Monitor and record changes in capacitance over time.

ii. Evaluate the strain-capacitance relationship using the electromechanical model of the SEC.

iii. Compare the data from direct painting and epoxy bonding methods.

1.1.4 Expected Results:

i. A detailed understanding of the advantages and limitations of the modified SEC design, especially with the extended SEBS polymer matrix.

ii. Comparative insights into the performance of direct painting versus epoxy bonding. One method might emerge as more suitable based on application needs.

iii. A potential solution to minimize capacitance coupling between the SEC and concrete, thereby improving strain detection accuracy.

iv. Recommendations on best practices for adhering SECs onto diverse substrates, ensuring longer sensor life and better efficiency.

1.1.5 Significance:

By enhancing the performance and reliability of SECs in SHM, this research will substantially contribute to ensuring structural safety and longevity. The findings will also be pivotal in expanding the applications of SECs across various industries and in diverse environmental conditions.

Chapter 2

Investigation of electrically isolated capacitive sensing skins on concrete to reduce structure/sensor capacitive coupling[1]

Abstract

Damage to bridges can result in partial or complete structural failures, with fatal consequences. Cracks develop in concrete infrastructure from fatigue loading, vibrations, corrosion, or unforeseen structural displacement. Effective long-term monitoring of civil infrastructure can reduce the risk of structural failures and potentially reduce the cost and frequency of inspections. However, deploying structural health monitoring (SHM) technologies for crack detection on bridges is expensive, especially long-term, due to the density of sensors required to detect, localize, and quantify cracks. Previous research on soft elastomeric capacitors (SEC) has shown their viability for low-cost monitoring of cracks in transportation infrastructure. However, when deployed on concrete for strain monitoring, a structure/sensor capacitive coupling exists that may cause a significant amplification in the signal collected from the SEC sensor. This work provides a detailed experimental study of electrically isolating capacitive sensing skins for concrete structures to reduce the structure/sensor

[1]Ogunniyi, E., Vareen, A., Downey, A. R., Laflamme, S., Li, J., Bennett, C., ... & Ziehl, P. (2023). Investigation of electrically isolated capacitive sensing skins on concrete to reduce structure/sensor capacitive coupling. Measurement Science and Technology, 34(5), 055113. https://doi.org/10.1088/1361-6501/acbb97. Reprinted here copyright for manuscript provided by publisher

capacitive coupling of an electrically grounded sensor. The study illustrates that the use of rubber isolators effectively decreases the capacitive coupling between concrete, which inherently has capacitive properties, and sensors such as the SEC that utilize capacitance measurements. In addition, the required thickness of isolation for accurate strain monitoring using the SEC with geometry described in the paper is investigated and better strain correlation is observed between the rubber of isolation thickness 0.30 mm and 0.64 mm with rubber of isolation of approximately 0.40 mm having the best response. Tests were conducted on small-scale concrete beams, and results were validated on full-scale reinforced concrete bridge decks recently taken out of service. This study demonstrates that with proper isolation material, the SEC can accurately transduce strain from concrete within a 10 $\mu\varepsilon$ error for strain levels beyond 25 $\mu\varepsilon$.

Keywords: capacitance strain sensor, structural health monitoring, sensing skins, flexible strain gauge, soft elastomeric capacitor, concrete strain.

2.1 Introduction

The deployment of structural health monitoring (SHM) technologies on bridges can be costly because numerous sensors are typically needed to gather a meaningful dataset across large surface areas. Moreover, geometrically complex structural details can be difficult to monitor with available sensing devices [11]. Smart sensing skins have been advantageous for continuous sensing over large areas [19, 26, 27], including surface sensors based on photonic crystals [28], carbon nanotube sensing skins [29], [30], damage sensitive paints [31], self-sensitive materials [32, 33], etc. Construction of *smart bridges* that incorporate particular sensors like strain gauge, corrosion sensors, and fiber-optic sensors [20] during construction is one of the most recent developments in SHM for bridges. However, the precision of these sensors may be constrained by environmental conditions such as humidity, wind, temperature, solar radiation, and

on-site construction defects at the job site [11].

The Soft Elastomeric Capacitor (SEC) is a sensing skin developed for mesoscale sensing that has been used both for fatigue crack detection in steel structures [15] and the reconstruction of full-field strain maps in structures [34]. Its relative cost, durability, and flexibility have made it a suitable sensor for large-area surface monitoring [35]. The SEC is a capacitive sensor attached to the structure being monitored with a thin layer of off-the-shelf epoxy. In-plane deformation in the structure (i.e., strain) produces a change in capacitance on the SEC. Changes in capacitance can be used to infer the structure's functionality when monitored over time. The strain on the monitored surface is obtained through the strain-capacitance relationship described in the electromechanical model of the SEC [15]. Of importance to this work are previous studies on the use of SEC for crack monitoring and detection; studies that investigate the use of SEC as strain sensing sheets on steel plates for crack detection report progressive data over the recent years [36, 37]. The studies have also been extended to strain sensing on concrete [38, 39].

Investigations on the concrete show that the SEC is sensitive to localized cracks on the concrete substrate [38]. However, strain values measured by the SEC are higher than the actual strain on the concrete being monitored. In order to utilize the soft elastomeric capacitors on concrete structures, it is essential to measure the actual strain present in the concrete, as opposed to simply monitoring abnormal variations (such as those caused by damage). In this work, it is hypothesized that high strains recorded by the SECs bonded on the concrete surface result from capacitance coupling between the SEC/concrete interface due to the intrinsic capacitance of the cement matrix in the concrete. [21]. Therefore, the challenge with deploying SECs on concrete is not because of the slight electrical conductivity of the concrete but rather its intrinsic capacitance. For example, the SEC has been successfully deployed on conductive materials such as aluminum and steel. The success of the SEC on

conductive materials is attributable to the fact that the impedance of these materials is nearly perfectly resistive. At the same time, concrete has a significant capacitive component to its impedance.

The authors introduce rubber as an isolation material between the SEC/concrete interface in this paper. Here, the thin rubber isolator eliminates unwanted electrical interference from the concrete on the SEC while allowing high-strain transmissibility. The contributions of this work are (1) extending previous research efforts on strain sensing on concrete by reducing capacitance coupling between the SEC and concrete using a rubber isolator, (2) investigating the performance of the SEC at different strain levels on concrete, and (3) providing an experimental investigation on capacitive coupling between a sensing skin and concrete structure. The paper is organized as follows. First, section 2 presents a background to the current study, including the SEC properties and electromechanical model. Next, section 3 expounds on the methodology, and the subsequent sections discuss the results and conclude the paper.

2.2 Background

2.2.1 Soft Elastomeric Capacitors (SECs)

The SEC is fabricated from a styrene-block-ethylene-co-butylene-block-styrene (SEBS) matrix where the sensor's dielectric is filled with titania (TiO_2) while its electrodes are doped with carbon black (CB) particles to make a conductive polymer. The manufacturing steps of the SEC are described in detail in prior work [40]. The SEC is a SEBS matrix, either filled or doped with additives to make a capacitor; the layers that make up the SEC have a robust mechanical connection since the electrodes and dielectric is made of the same polymer matrix (SEBS). In addition, the SEC's long-term weatherability has been demonstrated [41], making it an excellent candidate for long-term and low-cost monitoring of mesoscale structures. Figure 4.1 shows the schematic of a single SEC with a surface area of 76.2 $\times$ 76.2 mm (3 $\times$ 3 in). It is

worth noting that the geometry (such as form and size) can be changed. The resulting sensor has the following features: low cost, highly elastic, mechanical robustness, ease of installation, and low power consumption.

2.2.2 Electromechanical model

The SEC measures strain induced by deformations from the surface monitored. Deformations on the SEC result in an equivalent change in capacitance. Therefore, the SEC can be modeled as a parallel plate capacitor with the relationship in equation 3.1.

$$C = e_0 e_r \frac{A}{h} \tag{2.1}$$

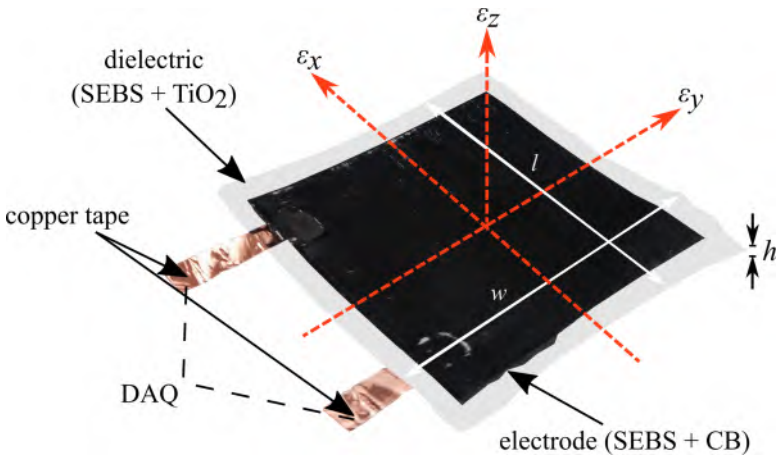

Figure 2.1 Sensing principle for a single SEC showing the schematic of the SEC including the dimensions and strain direction as measured by the SEC.

where $e_0 = 8.854pF/m$ is the vacuum permittivity, e_r is the dimensionless polymer relative permittivity, h is the thickness of the dielectric, and $A = l \cdot w$ is the sensor area where w is the width and l is the length as shown in figure 4.1. Changes in capacitance, ΔC, can be obtained by differentiating equation 3.1 (assuming small changes in strains on the monitored surface):

$$\frac{\Delta C}{C_0} = \left(\frac{\Delta l}{l_0} + \frac{\Delta w}{w_0} - \frac{\Delta h}{h_0}\right) = \varepsilon_x + \varepsilon_y - \varepsilon_z \tag{2.2}$$

ΔC denotes the capacitance change of the SEC due to strain, and C_0 represents the initial value of the SEC capacitance. ε_x, ε_y and ε_z are strains in the x, y and z directions, respectively. The SEC is deployed in the $x-y$ plane for surface strain monitoring. Assuming plane stress and applying Hooke's law,

$$\varepsilon_z = -\frac{\nu}{1-\nu}(\varepsilon_x + \varepsilon_y) \tag{2.3}$$

By substituting equation 3.3 into equation 4.2, a free-standing SEC has a capacitance response as,

$$\frac{\Delta C}{C_0} = \frac{1}{1-\nu_0}(\varepsilon_x + \varepsilon_y) \tag{2.4}$$

$$\frac{\Delta C}{C_0} = \lambda_0(\varepsilon_x + \varepsilon_y) \tag{2.5}$$

where ν_0 is Poisson's ratio for the SEC, and λ_0 is the SEC's gauge factor

In this paper, a gauge factor of 1.7 was used, experimentally validated in Liu et al. [42]. If ε_m is the strain on the monitored surface,:

$$\varepsilon_m = (\varepsilon_x + \varepsilon_y) \tag{2.6}$$

$$\frac{\Delta C}{C_0} = 1.7(\varepsilon_x + \varepsilon_y) \tag{2.7}$$

$$\frac{\Delta C}{1.7C_0} = \varepsilon_m \tag{2.8}$$

Equation 2.8 presents the relationship between nominal surface strain which is the measure of the deformation of the concrete specimen caused by an applied load; in this case, defined as the change in the length of the concrete divided by its original length and measured capacitance changes on SEC that can be used in structural monitoring.

2.2.3 Challenges associated with strain sensing on concrete

Strain sensing on concrete is associated with several inherent mechanical and electrical challenges. First, there are mechanical challenges with sensing strain on concrete due to its uneven, rough, and porous surfaces, resulting in issues when installing strain gauges on the surface. As a result, special preparations are required to ensure that strain on irregular concrete surfaces is fully transferred to strain gauges [43]. Furthermore, concrete is a heterogeneous material; the several components making up its structure can lead to the localization of stress and strain during loading, which can be a challenge when sensing strain with small sensors. However, the SEC's large size and simple installation process are sensor attributes well-suited for monitoring concrete.

Electrical challenges associated with SECs on concrete have been previously noted. For example, experimental results from Yan et al. [38] show that when an SEC sensor is attached to concrete, the measured strain values are significantly higher than anticipated. However, results by Yan et al. [38], and Downey et al. [39] show that when the exact amplitude of the signal is not considered significant but only the response to loading and damages is monitored, the general functionality of the SEC is not affected when used on concrete. The detection of crack formation can be inferred by monitoring an increase in the capacitance change of the SEC. Moreover, work by Laflamme et al. [40] has shown that the SEC can accurately transduce the dynamic signals in a modal test of a reinforced concrete beam. However, accurate strain monitoring of concrete using the SEC has not yet been demonstrated due to "amplification" in the SEC signal when attached directly to concrete. It is hypothesized that the amplification of the SEC's signal when adhered directly to the concrete is due to a complex capacitive coupling between the SEC and the intrinsic capacitance of the concrete. This hypothesis is tested throughout this work.

Several changes are expected to be seen as concrete undergoes mechanical de-

Table 2.1 Table showing rubber properties for natural rubber and neoprene.

Properties	Natural rubber	Neoprene
Durometer or Hardness Range	40 A	40 A
Poisson's ratio	0.48 - 0.5	0.46 - 0.49
Tensile Strength Range	($\geq$ 17237 kN/m^2)	5516 - 9653 kN/m^2
Elongation (Range %)	300 – 900%	100 – 800%
Temperature Range	93.3 - 200 °C	-34.4 - 121.1 °C

formations, including changes in intrinsic resistivity, change in bonding between the fillers and cement matrix, and change in capacitance [44, 45, 46]. These resulting changes pose challenges to external sensors attached directly to the concrete surface or inside the concrete. In particular, a few studies have demonstrated the intrinsic capacitance of concrete and how it varies with strain[45, 46]. For example, in concrete, capacitance-based strain sensing is based on piezopermittivity in which the permittivity of concrete increases upon compression, and vice versa under tension [45]. This can result in a 2 to 9% change in the capacitance of the measured concrete [46], which is hypothesized to interact with any capacitive-based sensors (i.e., SEC) mounted on the surface of the concrete.

Moreover, an investigation by Cheng et al. [47] detail how the size, position, and depth of rebar in the reinforced concrete beam affects the capacitance value recorded by a surface-mounted capacitance transducer. In addition, their results show that the corrosion of steel reinforcement affects capacitance values. Hence, using surface-mounted capacitance sensors like SECs to measure strain potentially faces challenges related to capacitive coupling.

2.3 Methodology

This section discusses the experimental procedure and materials for evaluation of the SEC for strain sensing on concrete.

2.3.1 Electrical isolation material

Natural rubber and neoprene with a durometer of 40A were selected as rubber isolators to investigate the SEC and concrete capacitance isolation. These two rubber isolators were selected because their Poisson ratios are close to 0.5, similar to SEC's Poisson ratio. Supplier-provided material properties are shown in table 2.1. Multiple thicknesses of the rubber isolators were investigated to determine the most efficient thickness of the rubber isolator that accurately described strain on the concrete specimen. For natural rubber, thicknesses of 0.203, 0.254, 0.305, 0.356, 0.508, 0.635, and 0.762 mm were investigated; for neoprene, 0.397, 0.793, 1.59, and 2.38 mm thickness were investigated. The installation of the rubber isolator to the concrete was done using a thin layer of off-the-shelf bi-component epoxy (JB Weld) to adhere it to the surface of the concrete before proceeding to install the SEC on the rubber isolator with the same epoxy.

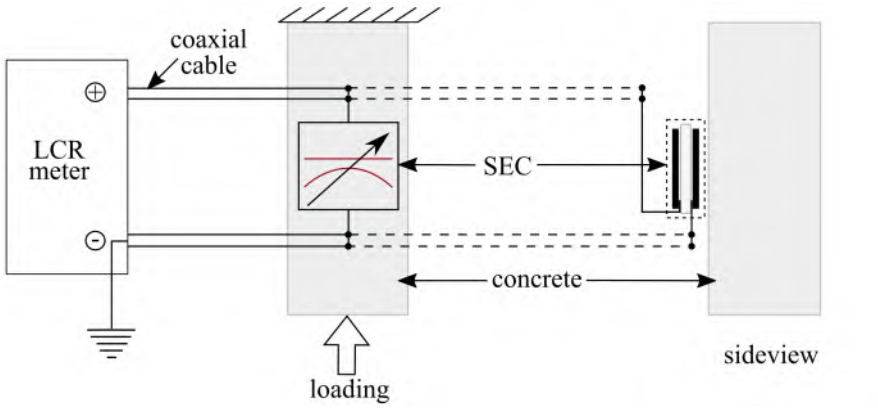

Figure 2.2 Circuit representation of the SEC as a variable capacitor adhered to the concrete sample with connection details.

A schematic representation of the SEC for strain sensing on concrete without an isolation layer between the SEC and concrete is shown in figure 2.2: the SEC is represented as a variable capacitor adhered to the concrete surface. The connection to the SEC's conductive plate attached directly to the concrete is grounded. However, this grounding does not reduce the structure/sensor capacitive coupling. As mentioned in

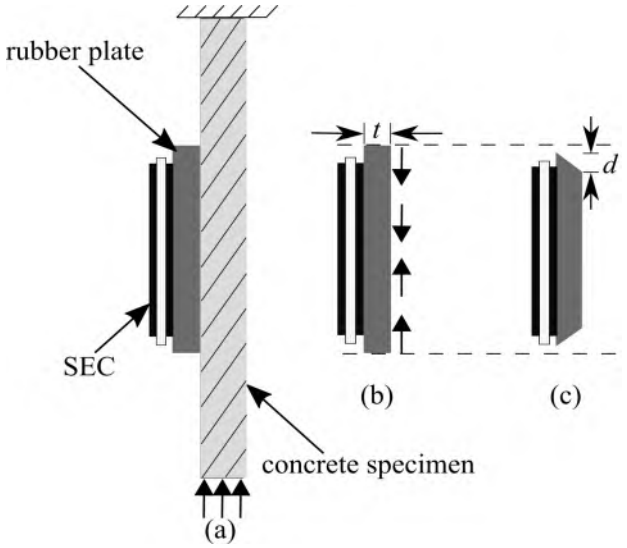

Figure 2.3 Deformation of the rubber isolating layer under a compression load showing: (a) diagram of the SEC and rubber isolator on the concrete surface; (b) SEC and rubber isolator without deformation with the arrows showing the strain direction, and; (c) SEC and rubber isolator after deformation.

the introduction, the overestimated strain signal obtained during testing led to further investigations on using rubber isolators between the SEC and concrete surfaces for capacitance decoupling.

Figure 2.3 reports the schematic representation of the strain transfer mechanism between the SEC and rubber isolator on the compressively loaded concrete specimen. The epoxy/bonding layers are thin and have a similar stiffness to the concrete, so their significance in the strain transfer mechanism can be ignored. The thickness of the rubber is denoted as t, and it is varied through the experimental process presented in this work. During the loading process, compressive strain in the concrete is transferred to the rubber isolator and then to the SEC. A thin layer of off-the-shelf epoxy is used to adhere the SEC to the rubber isolator as depicted in figure 2.3(b). This thin layer ensures that any variations in the rubber isolator are directly transmitted to the SEC. However, strain transmissibility from the concrete to the SEC through the rubber isolator depends on the thickness of the rubber and is explored in this work. Figure 2.3(c) shows the rubber isolator in a deformed state. It is hypothesized that as

the thickness t of the rubber isolator increase or decreases, d increases or decreases.

2.3.2 Data Acquisition and Processing

Capacitance data from the SEC were collected using an LCR meter (BK precision 891) with a driving frequency of 1 kHz, with a LabVIEW code to control the data acquisition process. The acquired capacitance data is related to strain according to the electromechanical model described in section 2. Data from a reusable surface-mount resistance bridge-based strain transducer (model ST350 manufactured by BDI) was acquired using a Bridge Analog Input (NI-9237 manufactured by NI). This reusable surface-mounted strain transducer is referred to as a "strain transducer" throughout this work. Load and displacement were acquired directly from the dynamic testing machine using an analog digitizer (NI-9239 manufactured by NI).

2.3.3 Testing procedure

Figure 4.3 shows the experimental setup used in this paper to investigate the concrete samples. Figure 4.3(a) shows a dynamic testing machine (MTS with Model No. 609.25A-01), having a maximum loading capacity of 250 kN. Compression tests were carried out to measure the SEC's compressive strain on a concrete specimen.

The concrete specimen is an unreinforced concrete section, with dimensions 0.305 $\times$ 0.102 $\times$ 0.102 m (4 $\times$ 4 $\times$ 12 in). The concrete was made using a 27 MPa (4000 psi) strength concrete mix, 3.5 L of water per 36.3 kg (80 lb) of concrete mix, and has an approximate density of 2014 kg/m^3 (125.73 lb/ft^3) on each sample. The specimens were allowed to cure for at least seven days before testing since only strain is acquired during the test, and the strength of specimens is not of priority. No changes in the concrete/sensor capacitive coupling were noticed with specimens allowed to cure for up to 6 months [38, 39]. In the exploratory stage of this study, more than 50 samples of concrete specimens were tested. To ensure consistency in the data, experimental

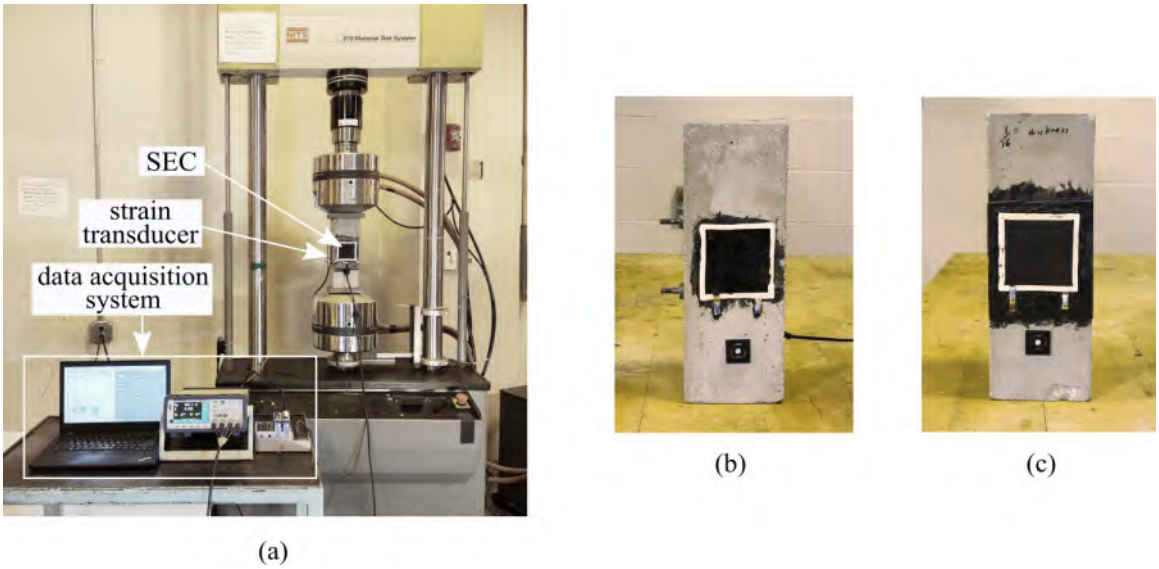

Figure 2.4 The specimen-scale testing experimental setup showing: (a) the concrete specimen on the dynamic testing system (MTS) with the data acquisition system which includes the NI DAQ and BK Precision 891 300 kHz; (b) the concrete specimen with SEC without isolation; (c) the concrete specimen with SEC with rubber isolator.

trials were repeated at various intervals of concrete curing with varying levels of humidity and grounding and shielding. However, the problem of capacitive coupling persisted in all test cases.

The cyclic loading procedure was designed to evaluate the performance of the SEC as a strain-sensing material on the concrete specimen, as shown in figure 3.3. The cyclic load was a 0.05 Hz harmonic excitation in fixed-compression mode between -22.5 and -45 kN. Strain data on the specimen-scale sample were obtained from the concrete using the SEC, strain transducer, and digital image correlation (DIC) during a steady-state cyclic loading condition. The concrete specimen was pre-loaded to -45 kN before strain data was acquired to prevent signal drift that is recorded during the initial loading. A drift in the SEC's signal was observed when the concrete specimen was initially loaded from a rest state, believed to be caused by electrical interference with the dynamic testing machine and in the initial settling of the concrete specimen under load. To compensate for this drift, the compression loading was started from a compressed state of -45 kN, as shown in figure 3.3.

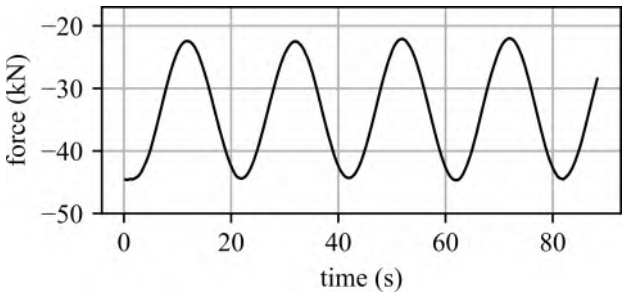

Figure 2.5 Loading profile for the concrete specimen showing the cyclic load between -22.5 kN and -45 kN.

The SEC and rubber isolator adhered to the surface of the concrete using the before-mentioned off-the-shelf bi-component epoxy after it was cleaned with sandpaper. During installation, the SEC was stretched slightly on all sides, of which the applied stretch to the SEC is about 2% of the original dimension on all sides to create initial strain on the SEC, allowing it to deform with the specimen. SEC installation on the full-scale concrete deck followed the same procedure. A coaxial cable was used to connect the copper tapes on the SEC to the data acquisition system for capacitance data acquisition. Special care is taken in cable management to ensure the cables do not move during testing.

Figure 2.6 shows the DIC setup used to observe the strain on the surface of the SEC, where the image focus and area of interest for strain evaluation are set on the SEC. This is done to compare the strain undergone by the SEC to the one measured directly by the SEC. In this work, a 5 MP camera controlled using VIC-snap from Correlated Solutions was used, and data were processed through VIC-3D. Strain data from the SEC, strain transducer, and DIC were obtained simultaneously using the previously described acquisition systems for each sensor. The results from the DIC measurements were also compared to the reference strain transducer measured values. For the DIC measurements, only the strain in the vertical direction ε_y, is considered for data processing.

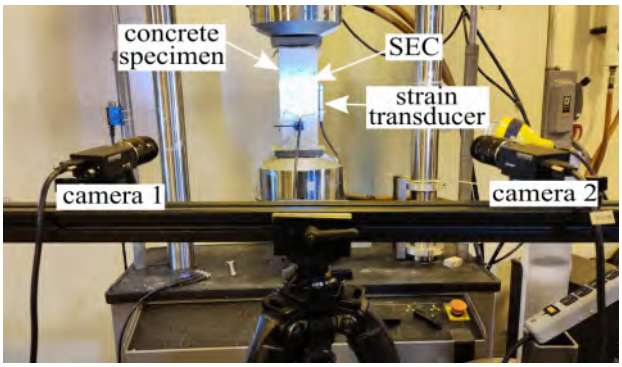

Figure 2.6 DIC experimental setup for strain data collection on the speckled concrete specimen.

2.3.4 Full-scale bridge deck evaluation

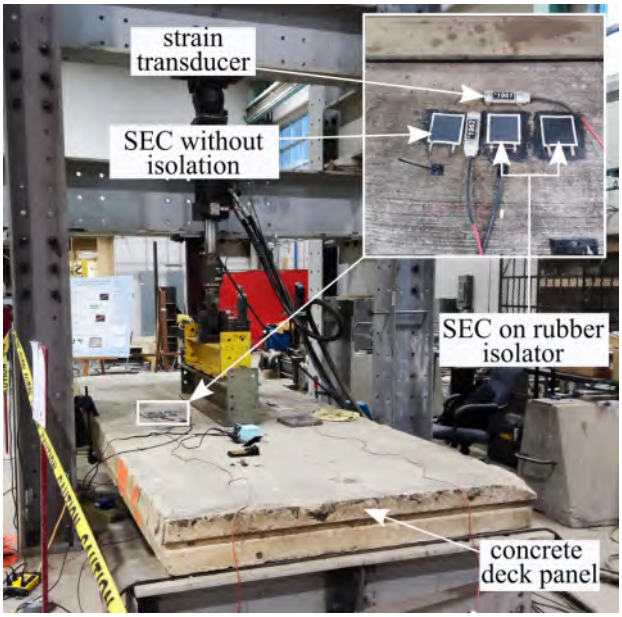

Figure 2.7 Experimental setup for full-scale reinforced concrete deck panel.

Experiments on the full-scale reinforced concrete bridge deck were performed to mimic an actual bridge's strain measurement. Figure 2.7 shows the setup for three-point bending of a full-scale reinforced concrete bridge deck with dimensions 4.27 × 1.52 × 0.23 m. This panel was removed from an in-service bridge deck and used to validate the SEC for monitoring strain on a real-world concrete structure. The loads introduced to the deck were controlled using a Shore-Western hydraulic actuator.

These unordered loads were applied to demonstrate the SEC response on a full-scale structure in the electrically noisy environment of a structures lab, simulating real-world conditions on a bridge. The SECs were installed on the bridge deck similarly to the small concrete specimens, and the same stretch of about 2% was applied during installation. The SEC and reference strain transducer were placed side by side at the center of the deck, where maximum strain is expected to be observed as shown in the inset of Figure 2.7.

2.4 Results and Discussion

This section explores the examination of several experimental trials that are conducted to assess the strain-sensing abilities of the SEC and the effectiveness of electrical isolators when used on concrete specimens.

The decibel signal-to-noise ratio ($\mathrm{SNR_{db}}$) and mean absolute error (MAE) from the data observed are calculated using equations 2.9 and 2.10, where z in equation 2.10 is the total number of samples collected. These calculations are used to determine the acceptability of the proposed use of a rubber isolator with SEC.

$$\mathrm{SNR_{dB}} = 10 \log_{10} \left(\frac{P_{\mathrm{signal}}}{P_{\mathrm{noise}}} \right) \tag{2.9}$$

$$\mathrm{MEA} = \frac{\sum_{i=1}^{z} |x_{\mathrm{true}_i} - x_{\mathrm{est}_i}|}{z} \tag{2.10}$$

2.4.1 Small-scale concrete specimens

Isolation of concrete specimen

Strain data from the compression tests show that the SEC measures a higher strain than the strain measured by the reference strain transducer. This disparity in

results where the SEC overestimates the strain in the concrete was repeatable and aligned well with data seen in prior research when the SEC was directly adhered to the concrete. The figure 2.8(a) displays the strain signal that has been amplified by the SEC. It is worth noting that the strain measurement obtained by the SEC closely aligns with the two widely used methods, DIC and strain transducer, in figure 2.8(b).

To study the effects using different capacitance measurement techniques, strain data were collected using two additional DAQs, both previously used successfully with the SEC. One DAQ was based on the PCAP02 capacitance-to-digital converter, which uses a time-constant measurement approach coupled with a time-to-digital converter [48]. Another was based on the FDC1004 capacitance-to-digital converter that uses a step waveform to excite the sensor and a sigma-delta analog-to-digital converter [49]. Results from both systems were the same as that observed with the BK Precision 891 LCR meter. The results support the hypothesis that the SEC/concrete capacitance coupling affects the SEC's strain sensing capacities, hence the need to isolate the two surfaces.

Figure 2.8(b) reports SEC strain data obtained using a 0.397 mm thick rubber isolator with the SEC. Strain data were also acquired using a strain transducer and digital image correlation (DIC). The data display a close correlation between the SEC, strain transducer, and DIC measurement, showing about 96% SEC strain accuracy when compared to the strain transducer, and about 94% accuracy when compared to the DIC measured data. In addition, the signal amplification observed in the test without isolation was eliminated, showing how a capacitive sensor's isolation enabled accurate strain monitoring on concrete.

DIC investigation of strain on the surface of SEC without isolation

DIC was used to investigate strain transmissibility through the SEC by investi-

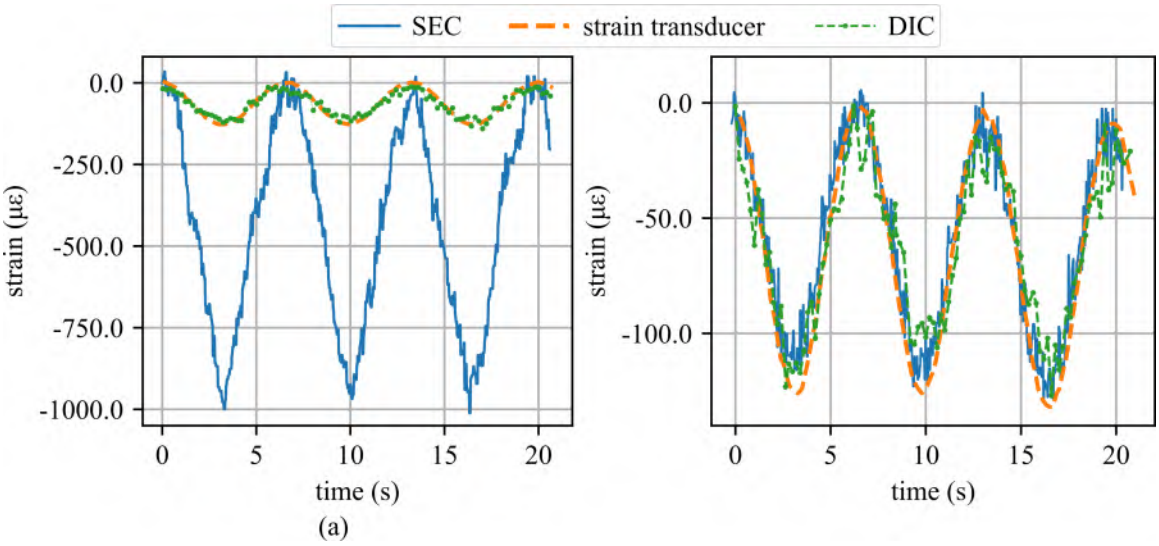

Figure 2.8 Strain results from SEC, strain transducer, and digital image correlation on (a) SEC adhered directly to concrete, showing the amplification of the SEC strain signal over the reference measurements; and (b) SEC signal using isolation with a rubber isolator of 0.397 mm thick.

Table 2.2 Strain data on concrete obtained from SEC, strain transducer, and DIC without isolation in the first 3.03 s of figure 2.8 (a).

time (s)	SEC ($\mu\varepsilon$)	strain transducer ($\mu\varepsilon$)	DIC ($\mu\varepsilon$)
0	0	0	0
0.63	-37.6	-17.9	-25.4
1.23	-247.6	-52.8	-57.7
1.83	-421.1	-86.9	-87.1
2.43	-684.2	-115.2	-96.6
3.03	-1004	-126.9	-110.1

gating strain on the outer surface of the SEC adhered to the concrete. The DIC investigation was done using the experimental setup shown in figure 2.6 by loading the concrete specimen with the described cyclic loading procedure. This study was done on the first 3 seconds of figure 2.8(a), where strain rises from 0 to -110 $\mu\varepsilon$ over 3.03 s.

The DIC strain data are shown in figure 2.9, where the distributed strain along the y-axis (ε_y)) on the surface of the SEC is shown from (a) - (f). Incremental strain is referenced from figure 2.9(a), therefore showing no strain at time 0 s. Figures 2.9(b) to (f) report strain data at equal time intervals of 0.6 s. A tensile strain of less than

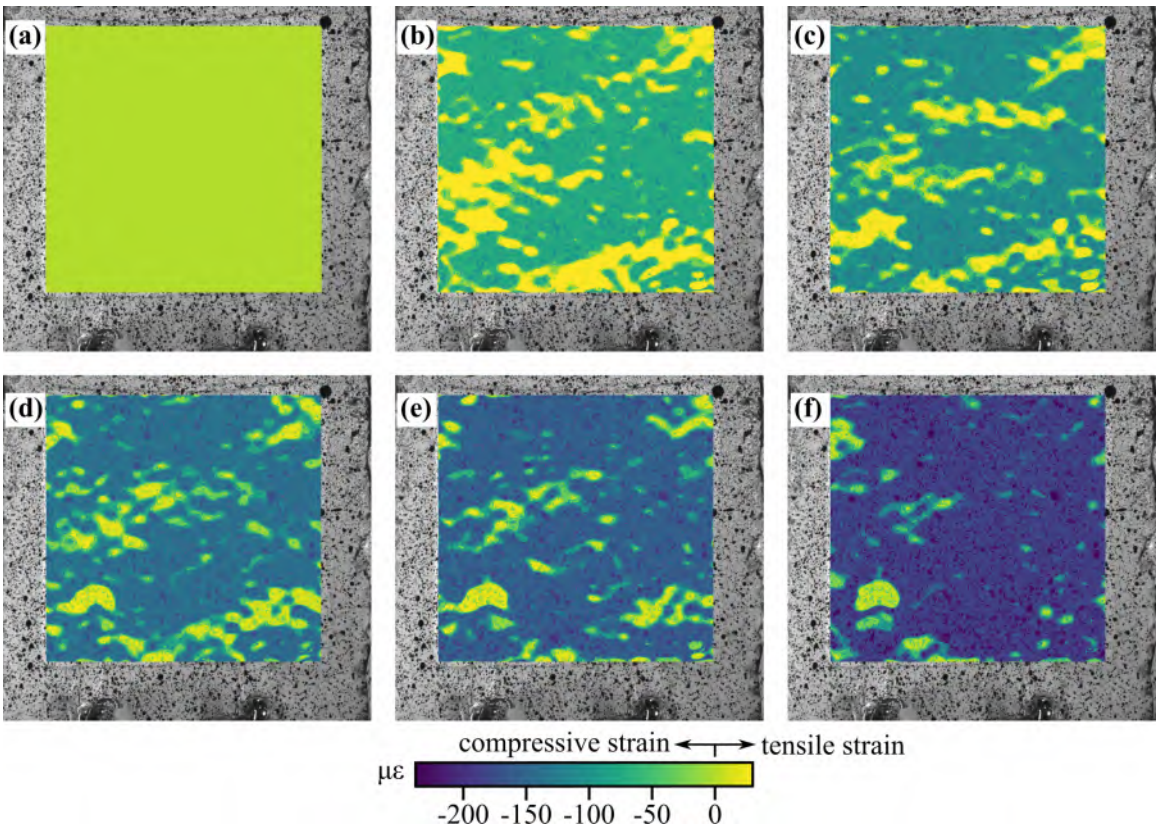

Figure 2.9 DIC measured surface strain in the SEC adhered to concrete without isolation under the loading shown in figure 2.8(a) at a specific time considered with: (a) at 0 s with a nominal strain value of 0 $\mu\varepsilon$; (b) 0.63 s with a nominal strain value of -25.4 $\mu\varepsilon$, and; (c) 1.23 s with a nominal strain value of -57.7 $\mu\varepsilon$, and; (e) 1.83 s with a nominal strain value of -87.1 $\mu\varepsilon$, and; (e) 2.43 s with a nominal strain value of -96.,6 $\mu\varepsilon$, and; (f) 3.03 s with a nominal strain value of -110.1 $\mu\varepsilon$, where the color bar indicates the strain at each point on the outer surface of the SEC with point 0 to the negative being compressive strain and 0 towards positive representing tensile strain.

25 $\mu\epsilon$ can be observed on the surface of SEC in Figure 2.9(b). The unevenness of the concrete causes this strain. As loading increases, the compressive strain becomes more prevalent.

Figure 2.9(f) shows the maximum strain recorded using the DIC. Note that the strain is not evenly distributed. However, the overall sum of the strain on the concrete is compressive at -110 $\mu\varepsilon$, compared to the SEC reported strain which is -1004 $\mu\varepsilon$ at the same time of 3.03 s. Table 2.2 details the strain measurements by the SEC, strain transducer, and DIC between 0 and 3.03 s. Table 2.2 confirms that the strains

measured by the strain transducer and DIC agree, while the SEC sensor overreports the strain.

Experimental testing of different isolation thickness

A study on the effects of the thickness of the rubber isolator is carried out to investigate the behavior of the SEC with different rubber isolator thicknesses for accurate strain sensing. Figure 2.10(a) to (k) reports the strain results with the use

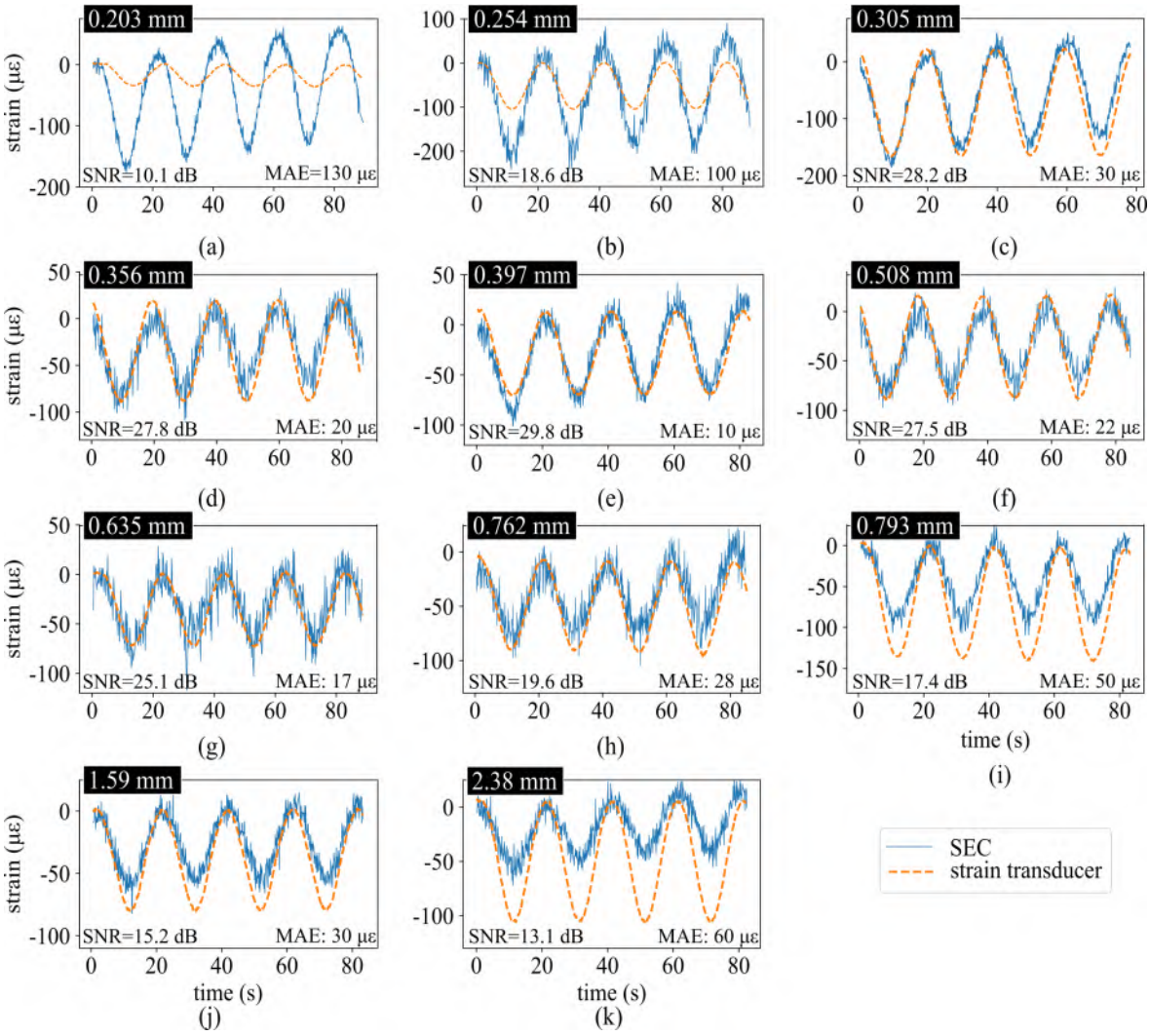

Figure 2.10 Strain data from use of different rubber isolator thickness for SEC/concrete isolation.

of different rubber isolator thicknesses, from 0.203 to 2.381 mm.

As the thickness of the rubber isolator increased to 0.305 mm figure 2.10(c), SEC and strain transducer data became better matched. However, the correlation began to decrease again after figure 2.10(g) with a rubber isolator of thickness 0.635 mm. Better strain correlation is observed between figure 2.10(c) at 0.305 mm to figure 2.10(g) at 0.635 mm, with each measured thickness having a high signal-to-noise ratio of at least 25. Furthermore, the signal-to-noise ratios presented in figure 2.11 shows that a rubber isolator with a thickness of 0.397 mm has the highest signal-to-noise ratio (SNR). The mean absolute error (MAE) is another metric used to assess the effectiveness of isolation thickness. The rubber thickness of 0.397mm has a lower MAE than other rubber insulators. These results support the hypothesis that adding the proper thickness of the isolation layer between the concrete and SEC decouples the capacitive interactions. However, the strain transmissibility through the electrical isolator becomes the limiting factor with increasing thickness.

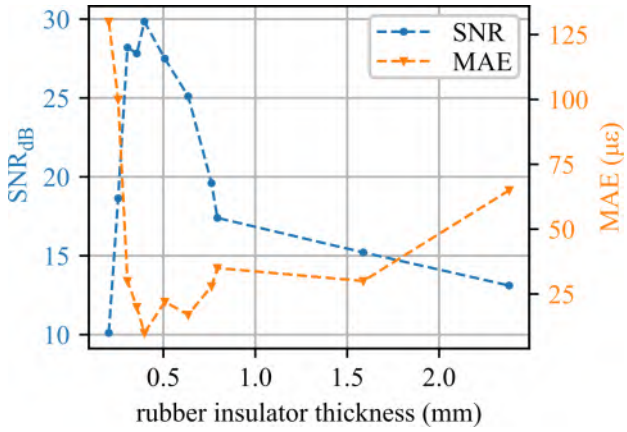

Figure 2.11 Signal to noise ratio of strain data of rubber isolator with varying thickness.

Strain range test with SEC on concrete

As reported in previous work, the SEC is best suited for 25 $\mu\varepsilon$ and above strain measurements. This is due to the relatively high noise in the measured signal. Figure 2.12 shows the strain measured by the SEC alongside the 0.397 mm rubber isolator and strain transducer as applied loading (strain level) was reduced. In this test, a rubber isolator with a thickness of 0.397 mm was chosen for use due to its superior performance in terms of signal-to-noise ratio (SNR) and lower mean absolute error (MAE) when compared to other rubber isolators that were evaluated. As shown, strain levels above approximately 25 $\mu\varepsilon$ can be accurately measured by the SEC. However, strain below 25 $\mu\varepsilon$ was affected by noise and will require a digital filter to digitize strain data from the SEC accurately. Note that the SEC can stretch up to 500% its original length in an unbounded configuration. Therefore, upper strain measurement in tension is limited by the concrete substrate, while its limit in compression strain measurement is limited by pre-tension applied to the SEC during installation on the structure.

Figure 2.13 reports the error in strain data from the SEC when compared to the reference strain data from the strain transducer. As indicated in the error plot, the clarity in the sensed strain is reduced at strain below 25 $\mu\varepsilon$. Therefore, using the SEC for sensing strain at 25 $\mu\varepsilon$ and above on concrete surfaces is advisable. Results are consistent with the 25 $\mu\varepsilon$ accuracy reported in previous work [35].

2.4.2 Full-scale testing

For the full-scale reinforced concrete deck panel test shown in figure 2.7, two rubber isolators of thicknesses 0.397 and 0.793 mm were tested. 0.397 mm was chosen due to its good signal-to-noise ratio demonstrated in the previous test in section 4.1, and 0.793 mm to show how a thicker isolation material affects strain sensing with the SEC. The SECs adhered to these two rubber isolators are investigated alongside an SEC directly adhered to the surface of the reinforced concrete deck panel to measure strain

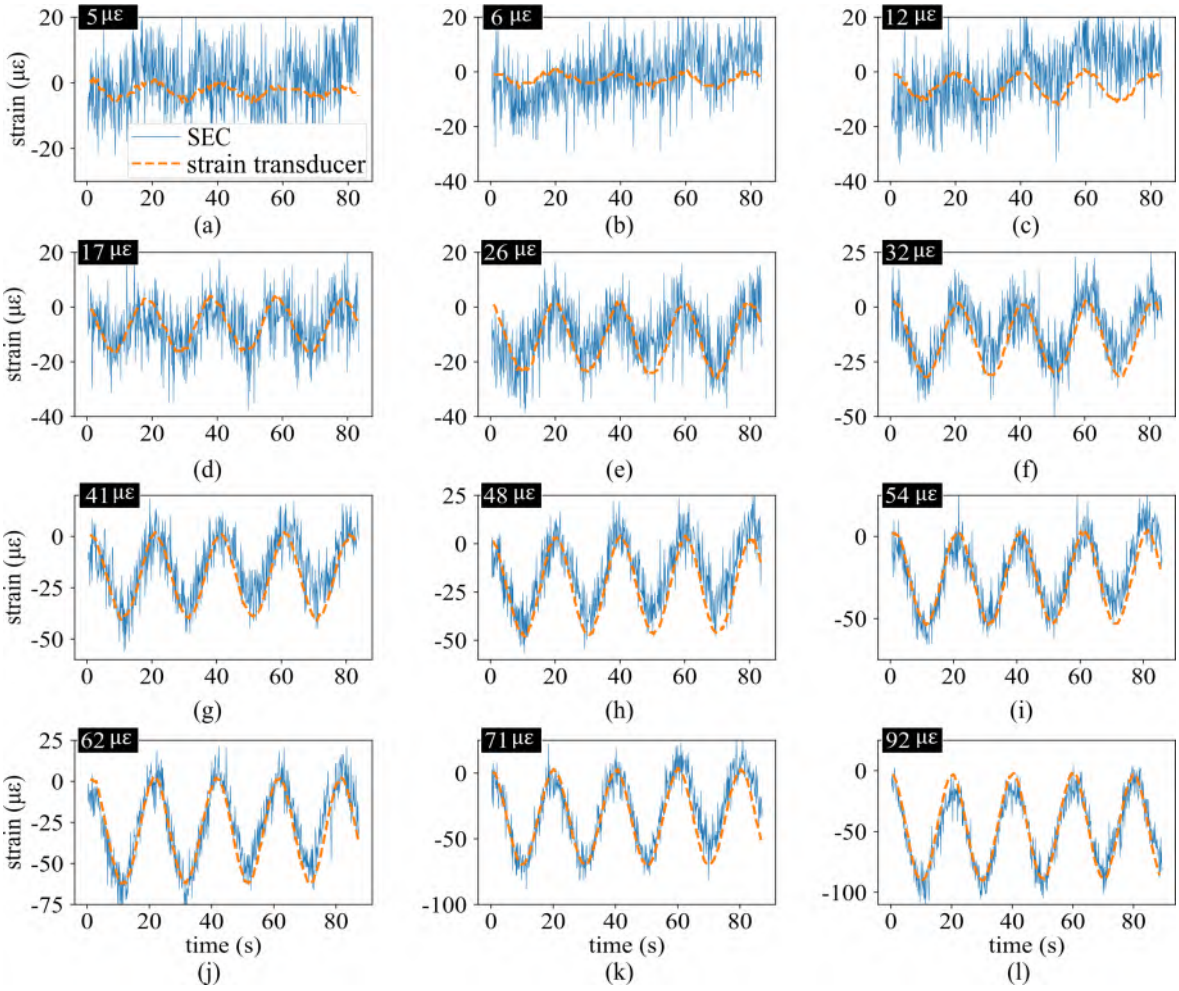

Figure 2.12 SEC Strain measurement obtained with a 0.397 mm rubber isolator for strain levels between 5 $\mu\varepsilon$ and 92 $\mu\varepsilon$.

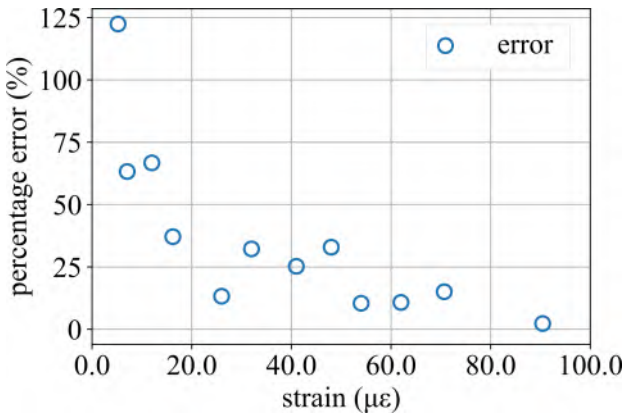

Figure 2.13 Percentage error for strain sensing at different strain levels with SEC.

data, as shown in the inset of figure 2.7. Two strain transducers were placed on the bridge deck to measure both horizontal and vertical strains, which, when combined, provide a total strain measurement by the strain transducer.

Figure 2.14 reports the temporal results for the full-scale test. Figure 2.14(a) reports the data for an SEC with no rubber isolator, and as expected, the SEC measured a higher strain value when compared to the strain transducer.

With the addition of a rubber isolator of thickness 0.397 mm, shown in figure 2.14(b), the SEC signal better aligns with that measured by the strain transducer. A similar result is observed in figure 2.14(c), where the rubber isolator of thickness 0.794 mm is used. In figure 2.14(c), a slight drift in the sensor signal is noticed after 80 seconds. However, the strain measured by the SEC is still better correlated with that from the strain transducer than the strain measured from the SEC directly adhered to the concrete. The result shows that a similar strain trend in the small-scale concrete sample is repeatable in full-scale reinforced concrete.

2.5 Conclusion

Using a soft elastomeric capacitance sensor (SEC), the study investigated strain sensing on concrete by introducing isolation materials at the SEC/concrete interface. Initial investigations show the need for an isolation material in the SEC/concrete interface for accurate strain measurement. This is because of the hypothesized capacitance coupling between the SEC and concrete, which results in an overestimated strain by the SEC. The use of isolation material at the SEC/concrete interface was found to effectively decreases the capacitive coupling between the concrete the SEC

Experimental investigations used rubber isolators as an isolation material at the SEC/concrete interface, and obtained strain data are compared to data from off-the-shelf strain transducers. The isolation data obtained are validated using digital image correlation. Strain measurements are repeated on a full-scale reinforced concrete

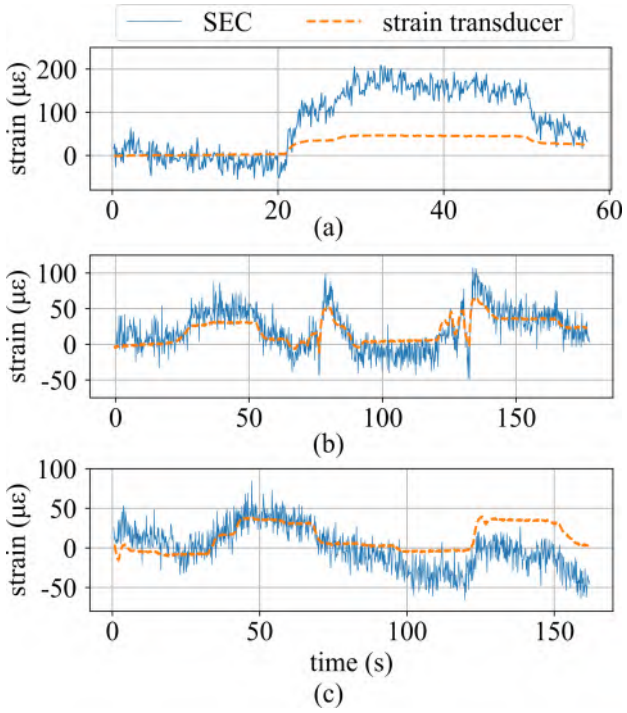

Figure 2.14 Strain data on full-scale reinforced concrete (a) without rubber isolator; (b) with rubber isolator of thickness 0.397 mm, and; (c) with rubber isolator of thickness 0.794 mm.

deck panel to mimic an actual bridge component. The results from the investigation showed about 96% SEC strain accuracy with the use of a rubber isolator with approximately 0.4 mm thickness.

When compared to off-the-shelf strain transducers, the SECs offer the ability to continuously monitor (spatial and temporal) large concrete structures. While off-the-shelf strain transducers for concrete surfaces provide good measurement quality; they can be expensive and difficult to maintain. Importantly when compared to the SEC, they do not cover large areas and therefore require a large number of sensors to provide distributed coverage of large structures like bridges. In addition, they are more sensitive to issues with bonding and surface preparation due to the point-wise installation of the sensors.

Further investigations showed that the SEC is more suitable for measuring strain at 25 $\mu\varepsilon$ and above on concrete. These results compare well to previous research

on using SECs to monitor strain on steel and composites. The investigations report improvement in strain data from the SEC and advise on the further development of the SEC for accurate strain sensing on concrete. Future research would investigate modifications to SEC to eliminate the need for isolation and the investigation of crack detection on concrete.

Acknowledgements

The authors gratefully acknowledge the financial support of the Departments of Transportation of Iowa, Kansas, South Carolina, and North Carolina, through the Transportation Pooled Fund Study TPF-5(449).

This chapter is wholly based on "Investigation of electrically isolated capacitive sensing skins on concrete to reduce structure/sensor capacitive coupling" published in Measurement Science and Technology, IOP Publishing 2023, doi: https://doi.org/10.1088/1361-6501/acbb97.

Emmanuel A. Ogunniyi[1], Alexander Vereen[1], Austin R.J. Downey[1,2] and Simon Laflamme[3,4], and Jian Li[5], and Caroline R Bennett[5], and William Collins[5], and Hongki Jo[6], and Alexander Henderson[2], and Paul Ziehl[1,2]

[1] Department of Mechanical Engineering, University of South Carolina, Columbia, SC 29201, United States

[2] Department of Civil and Environmental Engineering, University of South Carolina, Columbia, SC 29201, United States

[3] Department of Civil, Construction, and Environmental Engineering, Iowa State University, Ames, IA, United States of America

[4] Department of Electrical and Computer Engineering, Iowa State University, Ames, IA, United States of America

[5] Department of Civil, Environmental and Architectural Engineering, The University of Kansas, Lawrence, KS, United States of America

[6] Department of Civil, Architectural Engineering and Mechanics, The University of Arizona, Tucson, AZ,United States of America

Chapter 3

Soft elastomeric capacitors with an extended polymer matrix for strain sensing on concrete[1]

Abstract

Surface strain sensors, such as linear variable differential transformers, fiber Bragg gratings, and resistive strain gauges, have seen significant use for monitoring concrete infrastructure. However, spatial monitoring of concrete structures using these sensor systems is limited by challenges in the surface coverage provided by a specific sensor or issues related to mounting and maintaining numerous mechanical sensors on the structure. A potential solution to this challenge is the deployment of large-area electronics in the form of a sensing skin to provide complete coverage of a monitored area while being simple to apply and maintain. Along this line of effort, networks constituted of soft elastomeric capacitors have been deployed to monitor strain on steel and composite structures. However, using soft elastomeric capacitors on concrete surfaces has been challenging due to the electrical coupling between the sensors and concrete, which amplifies transduced strain signals obtained from the soft elastomeric capacitors. In this work, the authors investigate the isolation of the soft elastomeric capacitors from the concrete by extending the styrene-block-ethylene-co-butylene-block-styrene matrix of the soft elastomeric capacitors to include a decoupling layer between the electrode and the concrete. Experimental investigations are carried out on concrete specimens for which the soft elastomeric capacitor is adhered to with a thin layer of off-the-shelf epoxy

[1]Ogunniyi, E. A., Liu, H., Downey, A. R., Laflamme, S., Li, J., Bennett, C., ... & Ziehl, P. (2023, April). Soft elastomeric capacitors with an extended polymer matrix for strain sensing on concrete. In Sensors and Smart Structures Technologies for Civil, Mechanical, and Aerospace Systems 2023 (Vol. 12486, pp. 262-270). SPIE. doi: https://doi.org/10.1117/12.2658568. Reprinted here with permission of the publisher, 10/23/2023

and then loaded on the dynamic testing system to monitor strain provoked on the concrete samples. The results presented here demonstrate the viability of the electrically isolated soft elastomeric capacitors for monitoring strain on concrete structures. Initial comparisons between un-isolated and electrically isolated soft elastomeric capacitors showed that the nominal capacitance of the soft elastomeric capacitor is significantly lowered by adding an isolation layer of SEBS. Furthermore, strain results for the soft elastomeric capacitors are compared to ones from a resistive strain gauge and digital image correlation. The data obtained is significant for modifying soft elastomeric capacitors with the anticipation for future use on concrete structures.

Keywords: real-time model updating, high-rate dynamics, model reduction, eigenvalue modification, modal analysis, adaptive structures .

3.1 Introduction

Structural failures are primarily due to defective designs. However, several other factors have been identified that influence civil structure failures, such as faulty construction, foundation failure, extraordinary load, unexpected failure mode, and a combination of these causes [6, 7, 8]. While some of these causes are unavoidable, an excellent structural health monitoring (SHM) approach could prevent failures. The authors from references [9, 50, 51] expound on structural failures that result from precarious events, which lead to severe casualties, economic losses, and long-term risk for society. Therefore, understanding the behavior and performance of structures using effective structural health monitoring techniques is necessary to prevent these potential hazards [10]. Aside from public safety, researchers have demonstrated that SHM of civil structures has the potential to increase the life span of structures, lowers construction costs, enables early detection of risk, and improves the overall performance of the structure [11, 12].

Previous research efforts have investigated soft elastomeric capacitors for fatigue crack monitoring of steel. Soft elastomeric capacitors (SEC) have been used to monitor loads and fatigue cracks using the sensor's wireless network; the SECs are placed at strategic points on the bridge steel frame to monitor loading resulting from traffic [52]. Other investigations

using the SEC also include monitoring damages such as cracks on bridge structures [38]. The authors have previously extended research efforts to monitor strain on concrete structures by adhering the SEC directly to the surface of the concrete. The investigations by Ogunniyi et. al., [22] showed the need for electrical isolation of the concrete/sensor interface to prevent capacitive coupling between the SEC and the concrete; which leads to a capacitive signal that overestimates strain data. This is because concrete has innate capacitive properties while the SEC relies on capacitance measurements. The research demonstrated that using a rubber layer as an electrical isolation layer between the SEC and concrete is an effective way to reduce capacitive coupling.

Deploying the SEC with the use of additional isolation material is tasking, especially when installing multiple sensors. This work seeks to modify the SEC to achieve isolation by adding an extended polymer matrix of styrene-block-ethylene-co-butylene-block-styrene (SEBS) on both sides of the SEC sensor to act as an integrated isolation layer that extends the polymer matrix that makes up the SEC to five layers. The extended polymer matrix of SEBS is a transparent layer over the electrodes; this addition does not affect the sensor's sensitivity. With this design, a SEC is achieved for monitoring structural changes in concrete materials without needing separate isolation material.

This study evaluates the effectiveness of an extended polymer matrix on the SEC for measuring strains in concrete, building upon prior research in this area. In addition, the performance of the extended SEC is compared to that of commercially available resistive strain gauges and digital image correlation results. The contributions of this work are: 1) advancing previous research on strain sensing in concrete through the implementation of an extended polymer matrix of SEBS to minimize capacitance coupling between the SEC and concrete, and 2) conducting an experimental study on the capacitive coupling between a sensing skin and a concrete structure.

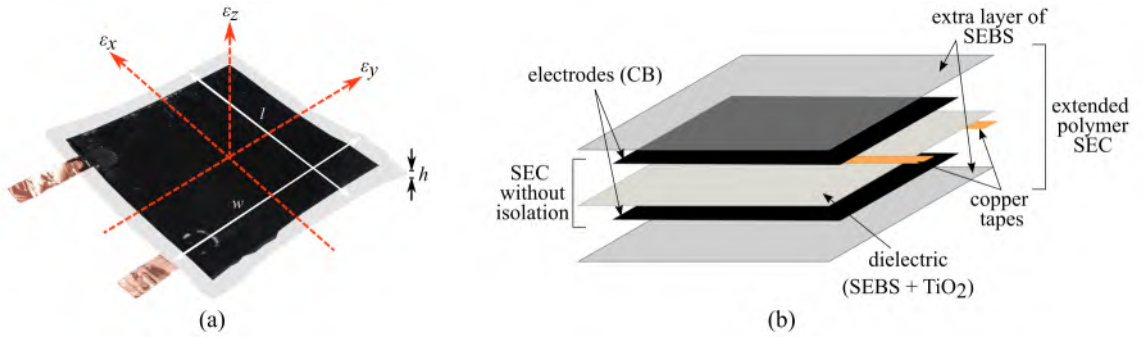

Figure 3.1 extended SEC where (a) shows the dry and ready-for-use sensor, and; (b) the schematic of the layers making up the extended sensor.

3.2 Background Studies

This section describes the SEC sensor and its electromechanical modeling.

3.2.1 SEC Sensor

An SEC is composed of a dielectric layer sandwiched between two electrodes. The dielectric is made up of a SEBS matrix that has been filled with titania (TiO_2), which is an inorganic particle improving the permittivity and durability of the SEBS matrix [53]. The electrodes are made of the same organic matrix as the dielectric layer, but they are doped with carbon black (CB) particles to make a conductive polymer. With properties like ultraviolet light stabilization and antioxidant capabilities, these CB particles were chosen to improve conductivity at a low cost while extending the polymer's life[54]. In addition, the layers that make up the SEC have robust mechanical interlayer bonding since the electrodes, and the dielectric is made of the same SEBS polymer matrix.

Figure 3.1(a) depicts a single SEC with a surface area of 76.2 × 76.2 mm (3 × 3 in), whereas Figure 3.1(b) depicts a schematic of the sensor with an extended polymer matrix proposed by this work. It is worth noting that the geometry (such as form and size) can be changed. The resulting sensor has the following features: low cost, great ultra flexibility, mechanical robustness, ease of installation, and low power consumption required for sensing.

3.2.2 Electromechanical model

The SEC utilizes the deformation induced by external forces on its surface to measure strain. As the SEC deforms, its capacitance also changes in proportion to the deformation. This behavior allows the SEC to be modeled as a parallel plate capacitor, as expressed by the following equation.

$$C = e_0 e_r \frac{A}{h} \tag{3.1}$$

where $e_0 = 8.854\text{pF}/m$ denotes the vacuum permittivity, e_r is the dimensionless polymer relative permittivity, h represents the thickness of the dielectric layer, and $A = l \times w$ is the sensor area, with w and l being the width and length, respectively, as depicted in Figure 3.1(a). Assuming small changes in strains on the monitored surface, the differential change in capacitance ΔC can be obtained by differentiating Eq.(3.1).

$$\frac{\Delta C}{C_0} = \left(\frac{\Delta l}{l_0} + \frac{\Delta w}{w_0} - \frac{\Delta h}{h_0}\right) = \varepsilon_x + \varepsilon_y - \varepsilon_z \tag{3.2}$$

ΔC denotes the capacitance change of the SEC due to strain, and C_0 represents the initial value of the SEC capacitance. ε_x, ε_y and ε_z are the strain in the x, y and z respectively. The SEC is deployed in the $x - y$ for surface strain monitoring. Assuming plane stress and applying Hooke's law,

$$\varepsilon_z = -\frac{\nu}{1-\nu}(\varepsilon_x + \varepsilon_y) \tag{3.3}$$

By substituting Eq.(3.3) into Eq.(4.2), the capacitance response of a free-standing SEC can be obtained:

$$\frac{\Delta C}{C_0} = \frac{1}{1-\nu_0}(\varepsilon_x + \varepsilon_y) = \lambda_0(\varepsilon_x + \varepsilon_y) \tag{3.4}$$

where v_0 is the Poisson's ratio for the SEC, and λ_0 is the SEC's gauge factor

$$\frac{\Delta C}{C_0} = \lambda_0(\varepsilon_x + \varepsilon_y) \tag{3.5}$$

The gauge factor used in this paper is 1.7, which has been experimentally validated [42].

$$\varepsilon_m = (\varepsilon_x + \varepsilon_y) \tag{3.6}$$

$$\frac{\Delta C}{C_0} = 1.7(\varepsilon_x + \varepsilon_y) \tag{3.7}$$

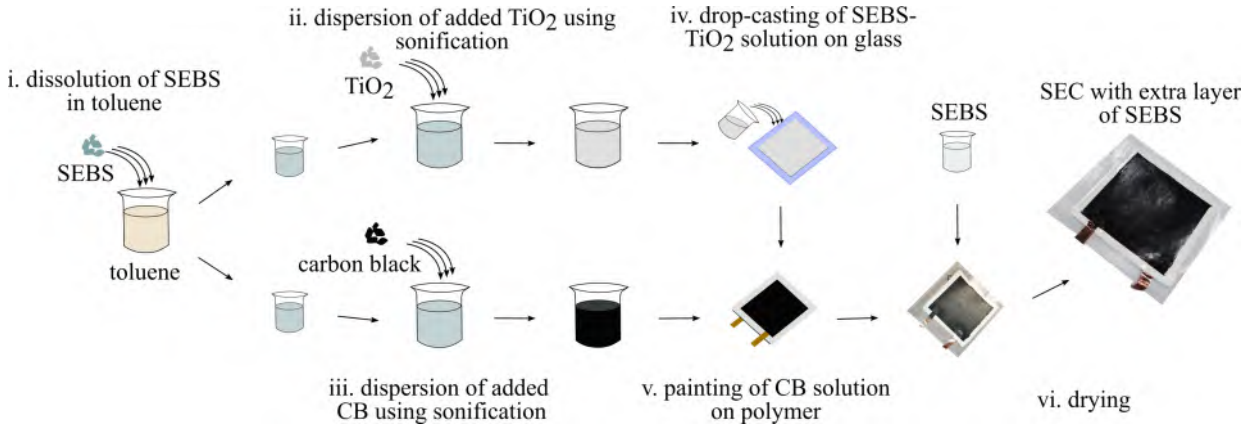

Figure 3.2 Extended SEC fabrication process.

$$\frac{\Delta C}{1.7C_0} = \varepsilon_m \tag{3.8}$$

where ε_m is the strain on the monitored surface.

3.3 Methodology

This section reports the fabrication procedure for the SEC with extended polymer matrix along with the experimental methodologies undertaken in this work.

3.3.1 Fabrication procedure for the SEC with extended polymer matrix

The process fabrication of the SEC with extended polymer matrix (Figure 3.1(b)) is described below, diagrammed in Figure 3.2, and broken down into the six steps that follow.

i. Toluene is used as the solvent to dissolve SEBS 500120M (Mediprene Dryex) particles to prepare the SEBS/toluene solution at a concentration of 160 g/L. PDMS-coated titania TiO_2 (-OSI$(CH_3)_2$-) rutile particles are dispersed in a portion of the SEBS/-toluene solution at a concentration of 75 g/L.

ii. Titania particles are further uniformly dispersed in the SEBS matrix using an ultrasonic tip (Fisher Scientific D100 Sonic Dismembrator) at 20 kHz and 120 watts for 5 minutes.

iii. Another SEBS/toluene solution is prepared by dissolving SEBS 500050M in toluene for a concentration of 380 g/L. CB particles (Orion Printex XE 2-B) are scattered at

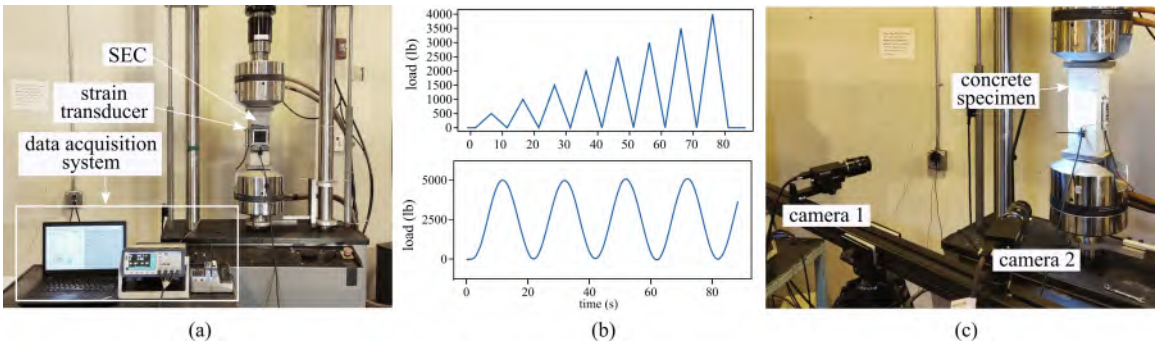

Figure 3.3 The specimen-scale testing experimental setup showing: (a) the concrete specimen on the dynamic testing system with the data acquisition system which includes the NI DAQ and BK Precision 891 300 kHz; (b) the loading procedure used in the experimental process, and; (c) DIC experimental setup for the strain data collection on the speckled concrete specimen.

a 25g/L concentration in the stock solution and dispersed using a low-speed homogenizer for one hour at 650 rpm.

iv. The dielectric layer is made utilizing a solution cast process, in which 20 ml of the prepared SEBS-TiO2 solution is dropped and cast directly onto a 76.2 × 76.2 mm (3 × 3 in) glass slide and covered for 24 hours in the fume hood to allow toluene to evaporate. The resulting film is peeled off from the glass plate and left to dry for 12 hours at room temperature.

v. The resulting SEBS-CB solution is brushed onto both the top and bottom surfaces of the dielectric, and a total of 4 layers of the conductive solution are brushed on each side with 30 minutes of drying between each layer. Two conductive copper tapes are implanted into the liquid electrode layers to provide mechanical connections for the wires that connect the sensor to the data acquisition system.

vi. The resulting multi-layer nanocomposite is allowed to dry for 24 hours. The SEC is then extended with an extra layer of nonconductive SEBS 500120M/toluene solution without TiO_2 on both surfaces for a composite configuration, preventing capacitive coupling between the electrode and the concrete layer.

3.3.2 Experimental Setup

Figure 3.3 illustrates the experimental setup employed in this study to examine the concrete samples. The concrete specimen is loaded using a dynamic testing device (MTS Model No. 609.25A-01) capable of supporting up to 250 kN of load, as shown in Figure 3.3(a).

The compressive tests were conducted on an unreinforced concrete specimen with dimensions of 0.305 × 0.102 × 0.102 m (4 × 4 × 12 in), manufactured using 3.5 L of water per 80 kg of a 27 MPa (4000 psi) strength concrete mix. The density of each sample was approximately 2014 kg/m3 (125.73 lb/ft3). To ensure reliable strain measurements, the surface of the concrete was scrubbed with sandpaper and cleaned thoroughly before the SEC was bonded to it using off-the-shelf bi-component epoxy. A stretch of about 2% of the initial dimension was applied to the SEC during installation to place it under initial strain, allowing it to deform along with the specimen during testing.

The performance of the SEC as a strain-sensing material on the concrete specimen was evaluated using a triangle and cyclic loading process, as illustrated in Figure 3.3(b). The loading was fixed-compression mode harmonic excitation at 0.05 Hz and ranged from 0 to 4000 lb. In addition, strain measurements on the concrete sample were collected under steady-state cyclic loading conditions using the SECs, strain transducer, and digital image correlation (DIC).

Capacitance values from the SEC were obtained by using an LCR meter (BK precision 891) with a drive frequency of 1 kHz and LabVIEW code to manage the data acquisition procedure. The collected capacitance values were then related to strain using the electromechanical model given in section 2. Data from a reusable surface-mount resistance bridge-based strain transducer (BDI ST350 model) was collected using a bridge analog input module (NI-9237 manufactured by NI), while load and displacement were acquired from the dynamic testing apparatus using an analog digitizer (NI-9239 manufactured by NI).

A DIC setup was employed to validate the strain on the surface of the SEC, as shown in Figure 3.3(c). The SEC was the image focus and area of interest for strain measurement, and image data from a 5 MP camera was analyzed using VIC-3D from Correlated Solutions.

3.4 Results and Discussion

The following section presents an analysis of the findings from the study, including a discussion of the application and interpretations of the results.

3.4.1 Sensor nominal capacitance

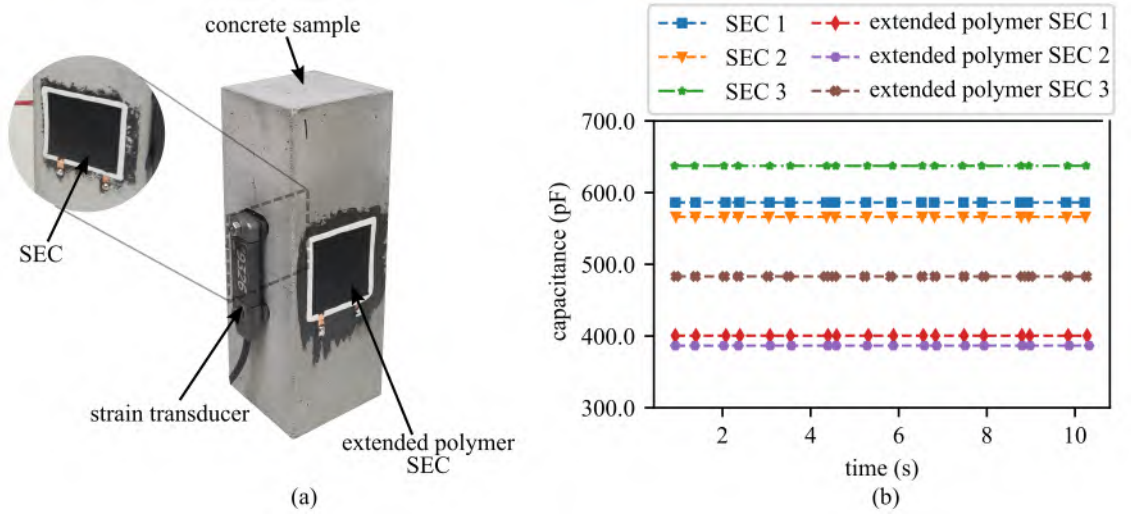

Figure 3.4 Shows (a) concrete specimen with SEC, extended layer SEC and strain transducer attached to it, and; (b) shows the nominal capacitance of the SECs upon adhering them to the concrete specimens.

The introduction of isolation on the SEC in the form of an extra layer of SEBS alters the nominal capacitance of the SEC. The extra layer of SEBS added to the SEC also increased

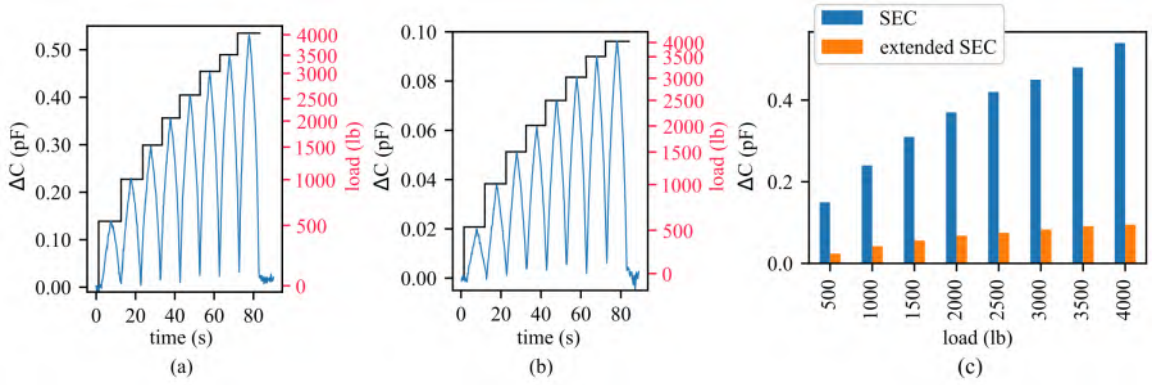

Figure 3.5 Capacitance change in response to load observed using (a) SEC; (b) extended SEC, and; (c) both sensors.

the thickness of the sensor, therefore adding to the stiffness of the SEC. Increasing the SEC stiffness lowers its nominal capacitance. Figure 3.4(a) shows the SEC, extended layer SEC and strain transducer on the surface of the concrete, and Figure 3.4(b) shows the nominal capacitance of both SEC upon adhering them to the concrete surface. For the six SECs sample observed, the SECs without an extra layer of SEBS have higher nominal capacitance compared to ones with an extra layer of SEBS.

Responses to loading

The SECs were subjected to increasing triangle loading as shown in fig 3.3(b), and capacitance change to load in both SEC is shown in Figure 3.5(a) and (b). As seen in both sensors' responses to load, the capacitance change decreases as the incremental load increases from 500 to 4000 lb at an increment of 500 lb. Figure 3.5(a) shows the response of the SEC to incremental load. The first 500 lb load increment causes a 0.14 pF change in the nominal capacitance of the SEC. However, compared to Figure 3.5(b), which is the capacitance change for the extended SEC, the first 500 lb load addition resulted in a 0.02 pF change in capacitance. The subsequent addition of a 500 lb load measured by both sensors showed a similar trend. Equal load resulted in a bigger capacitance change in the SEC compared to the extended SEC as shown in the barplot of Figure 3.5(c). Adding an extra layer of SEBS to the SEC greatly reduces the capacitive coupling that results an overestimated measurement in the SEC.

3.4.2 Strain results

Strain data were acquired from three concrete specimens subjected to compressive loads using an SEC, an extended SEC, and a strain transducer. Figure 3.6 display the strain obtained from the three samples. As observed in the three samples, the strain measured by the SEC is higher than the other two sensors, and the strain from the extended SEC closely agrees with the one measured by the strain transducer. Therefore, the strain measured by the SEC is overestimated compared to the actual strain in the concrete specimen; as discussed in detail in reference [22].

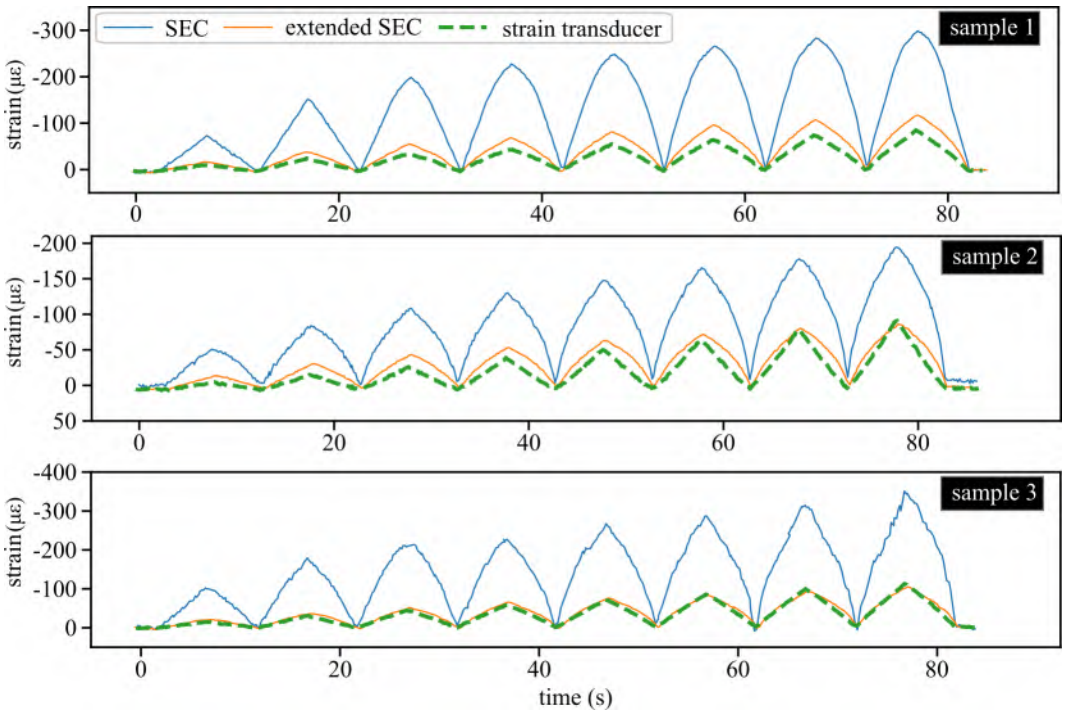

Figure 3.6 Strain measured from three concrete specimens using SEC, extended SEC, and strain transducer.

The strain on the SEC's surface bonded to the concrete was examined using digital image correlation for one sensor. The concrete specimen was loaded using the described cyclic loading method as part of the DIC investigation utilizing the experimental setup indicated in Figure 3.3(c). The strain map for the first 6.03 s of Figure 3.7(a) is shown in Figure 3.7(b) at an interval of 0.6 s. The DIC strain data displays the distributed strain along the y-axis (ε_y)) on the surface of the SEC. Maximum strain is observed at 3.03 s where the DIC recorded a strain of -82 $\mu\varepsilon$, the SEC measured a strain of -376 $\mu\varepsilon$, while the extended SEC measured a strain of -112 $\mu\varepsilon$. This data confirms that the strains measured by the extended SEC and DIC are close, while the SEC overreports the strain.

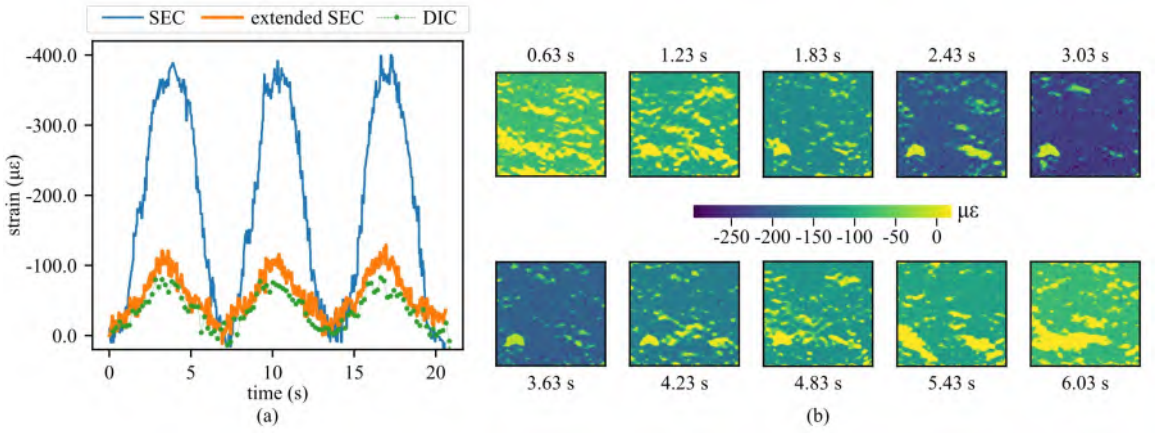

Figure 3.7 Detailed DIC investigation for strain data obtained from a sensor, showing: (a) data obtained from an SEC, extended SEC, and digital image correlation, and; (b) strain map from the digital image correlation from 0.63 s to 6.03 s at an interval of 0.6 s.

3.5 Conclusion

This study investigated using an extended soft elastomeric capacitor (SEC with an extra layer of SEBS) on concrete. This extra layer was added to minimize the capacitive coupling between the SEC and concrete, which results in overestimated measurements, as observed in previous research efforts. The paper observed the response to loading for the SEC and the extended SEC by comparing the relative capacitance change in both sensors under the same load. This investigation shows that the SEC without extra layers of SEBS has a higher capacitance change for each change in loading than the SEC with extra layers of SEBS.

Strain data obtained from the capacitance change in both SECs and the off-the-shelf strain transducer showed that the strain data from the extended SEC and strain transducer are more closely aligned. Further validation of strain data was carried out using digital image correlation, which also showed that the extended SEC is viable for strain measurements on concrete structures. The investigations report improvement in strain data from the SEC when used on concrete surfaces, and future research will focus on applications for measurements on concrete structures.

Acknowledgments

The authors gratefully acknowledge the financial support of the Departments of Transportation of Iowa, Kansas, South Carolina, and North Carolina, through the Transportation Pooled Fund Study TPF-5(449).

This chapter is wholly based on "Soft elastomeric capacitors with an extended polymer matrix for strain sensing on concrete" published in SPIE Proceedings, 2023, doi: https://doi.org/10.1117/12.2658568.

Emmanuel A. Ogunniyi[1], Han Liu[3], Austin R.J. Downey[1,2] and Simon Laflamme[3,4], and Jian Li[5], and Caroline R Bennett[5], and William Collins[5], and Hongki Jo[6], and Alexander Henderson[2], and Paul Ziehl[1,2]

[1] Department of Mechanical Engineering, University of South Carolina, Columbia, SC 29201, United States

[2] Department of Civil and Environmental Engineering, University of South Carolina, Columbia, SC 29201, United States

[3] Department of Civil, Construction, and Environmental Engineering, Iowa State University, Ames, IA, United States of America

[4] Department of Electrical and Computer Engineering, Iowa State University, Ames, IA, United States of America

[5] Department of Civil, Environmental and Architectural Engineering, The University of Kansas, Lawrence, KS, United States of America

[6] Department of Civil, Architectural Engineering and Mechanics, The University of Arizona, Tucson, AZ,United States of America

Chapter 4

Enhancing Structural Health Monitoring with direct coated Carbon Black on monitored surface for Elastomeric Capacitors adhesion

This chapter is discusses the methodology for adhering the soft elastomeric capacitors on the monitored surface, and the resulting performance of a selected approach

Abstract

Soft elastomeric capacitors (SECs) are promising sensors with applications in structural health monitoring, environmental sensing, and human-machine interaction. However, adequate adhesion onto diverse surfaces, such as concrete and metals, could significantly affect their sensing capabilities. This paper studies two methods of adhering soft elastomeric capacitors to monitored surfaces: direct painting with carbon black (CB) and epoxy bonding. This study's significance lies in adhesion's critical role in ensuring accurate and reliable sensor performance. SECs can provide valuable real-time data on strain or deformation, making them indispensable for several applications. By investigating direct painting and epoxy bonding techniques, we seek to study effective method for achieving robust and durable adhesion, maximizing the sensor's lifespan and performance. The preliminary steps in this study involve the fabrication of the SECs and the preparation of monitored surfaces for adhesion. Some SECs were directly painted on the monitored surface using carbon black, while some were adhered using an off-the-shelf epoxy. These monitored surfaces were tested under mechanical stress and deformation to evaluate the sensor's performance. The parameters considered for analysis include adhesion strength, electrical conductivity,

and overall sensor functionality. CB-painted SECs are simple and cost-effective, facilitating quick sensor deployment. However, its performance may degrade due to wear and tear, limiting its long-term durability. Conversely, epoxy bonding demonstrates exceptional adhesion strength and stability, ensuring prolonged sensor functionality, but may require more intricate fabrication processes. Through a investigation of these adhesion methods, this study provides valuable insights into selecting the most appropriate technique for specific applications. Furthermore, it contributes to optimizing soft elastomeric capacitors' adhesion on concrete and metal surfaces, paving the way for enhanced sensor performance and widespread implementation in various industries.
Keywords: soft elastomeric capacitors, adhesion methods, direct painting, epoxy bonding, concrete, metal surfaces, structural health monitoring, sensor performance.

4.1 Introduction

Soft elastomeric capacitors(SECs) have emerged as versatile sensors with tremendous potential for diverse applications, ranging from structural health monitoring to environmental sensing and wearable electronics [13, 14, 15]. Their unique properties, such as high flexibility, conformability, and the ability to measure strain, pressure, and deformation, have rendered them indispensable in modern engineering and healthcare domains [55, 56]. However, the effective integration and adhesion of these soft elastomeric capacitors onto various monitored surfaces, such as concrete and metals, remain an area of concern for efficient monitoring.

Over the years, the SEC has been continuously improved to achieve optimal performance when used for monitoring changes on a surface. Of its several applications, the soft elastomeric capacitors has proven significantly beneficial in bridge structural health monitoring (SHM) [16], fatigue crack detection and monitoring [57], on-human applications [17, 18] and much more [58]. Efforts to achieve a robust and high-performing sensor has been seen in modifications to the SEC design over the years from the addition of texture/-corrugation to the SEC [59], adding extra polymer layer of SEBS to out layer of the SEC to prevent capacitive coupling between the SEC [23, 24] and concrete surface to Paintable

Silicone-Based Corrugated SECs for Area Strain Sensing [60]. The mode of adhering the SECs to the monitored surface in previous use has been with an off-the-shelf bi-component epoxy, however, the transfer effectiveness of the epoxy layer is somewhat questioned.

To ensure optimal sensor performance and longevity, the adhesion of soft elastomeric capacitors to their respective substrates is of paramount importance. This paper present a comprehensive study on two distinct methods for adhering soft elastomeric capacitors to concrete and metal surfaces: direct painting and epoxy bonding. The aim of this investigation is to identify the most effective adhesion technique that ensures robust and reliable sensor functionality based on the testing conditions. The significance of this study lies in the critical role of adhesion in determining the overall performance of soft elastomeric capacitors in practical applications. Their accurate and consistent measurements of mechanical and environmental parameters are crucial for structural health monitoring in civil engineering, human-machine interaction, and bio-signal sensing in healthcare devices. However, improper adhesion can lead to delamination, reduced sensitivity, and the loss of electrical contact, compromising the sensor's efficiency and lifespan [25, 61].

Direct painting, a straightforward and cost-effective method, involves applying the elastomeric material directly onto the surface of interest. While this approach simplifies the fabrication process and expedites sensor deployment, concerns arise over its long-term stability and durability in demanding environmental conditions . Epoxy bonding, on the other hand, entails the use of specialized adhesives to firmly attach the soft elastomeric capacitor onto the substrate. This technique offers exceptional adhesion strength and robustness, which is particularly beneficial for harsh environments and extended monitoring applications.

Ultimately, this study aims to optimize the adhesion of soft elastomeric capacitors on concrete and metal surfaces, enhancing their performance and reliability in practical applications. The findings presented herein will be crucial in advancing the field of soft sensors and promoting their integration into diverse industries and technologies. The paper is organized as follow, In this paper, we outline the experimental methodology used to fabricate soft elastomeric capacitors and prepare concrete and metal surfaces for adhesion. The com-

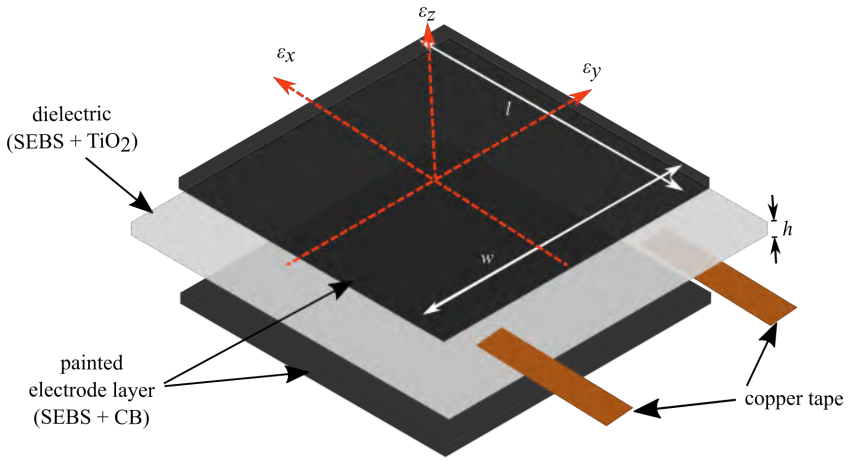

Figure 4.1 extended SEC where (a) shows the dry and ready-for-use sensor, and; (b) the schematic of the layers making up the extended sensor.

parative analysis of the direct painting and epoxy bonding methods includes assessments of adhesion strength, electrical conductivity, and sensor functionality over an extended period of testing. The results of these investigations will contribute to the understanding of each adhesion technique's merits and limitations, thereby guiding the appropriate selection of method based on specific application requirements.

4.2 Background

4.2.1 Overview of soft elastomeric capacitors and their applications

Soft elastomeric capacitor (SEC), a flexible and deformable capacitive sensor, have gained considerable attention in recent years due to their unique properties and diverse applications. These soft sensors typically comprise elastomeric materials with embedded conductive elements, making them sense mechanical deformations and environmental changes.

The sensing mechanism of soft elastomeric capacitors relies on changes in capacitance resulting from mechanical strain or deformation applied to the elastomeric material [62]. When subjected to external forces, the distance between the conductive elements within the elastomer changes, leading to variations in the capacitance of the sensor. Consequently, this change in capacitance can be correlated to the magnitude of the applied mechanical stress, enabling accurate and real-time sensing of physical parameters.

The choice of elastomeric materials is critical in the design of soft capacitive sensors, as it directly influences their flexibility, conformability, and sensitivity. Silicone-based elastomers, such as polydimethylsiloxane (PDMS), are commonly employed due to their excellent mechanical properties and biocompatibility [63]. Other elastomers, like thermoplastic polyurethane (TPU) and elastomeric composites, have also been explored to tailor the sensor's characteristics for specific applications [64]. The production process of the SEC employed in this work is discussed by Liu et al. [57].

Soft elastomeric capacitors find extensive applications in various fields due to their adaptability and versatility. Its usage is not limited to Structural Health Monitoring (SHM), Wearable Electronics, Human-Machine Interaction (HMI), Environmental Sensing, Biomedical Sensing, and Internet of Things (IoT) Devices.

Soft elastomeric capacitors offer several advantages over conventional rigid sensors, including lightweight, conformability to irregular surfaces, and enhanced user comfort. Their flexible nature enables seamless integration into curved and complex geometries, making them suitable for unconventional and hard-to-reach areas. Additionally, using elastomeric materials enhances the sensor's robustness and resistance to mechanical stress.

4.2.2 SECs electromechanical model

Figure 4.1(a) shows an SEC featuring a reinforced diagrid pattern. The fundamental principle of strain sensing is the sensor's alteration in area (i.e., strain) (induced by strain on the monitored surface) to a quantifiable change in capacitance. This can be derived by considering the initial capacitance (C_0) of a non-lossy parallel plate capacitor:

$$C_0 = e_0 e_r \frac{A}{h} \tag{4.1}$$

The relative change in capacitance ($\Delta C/C_0$) can be determined by differentiating Equation 4.1, considering small strains along the x-direction. In this equation, $e_0 = 8.854pF/m$ represents the vacuum permittivity, e_r denotes the relative permittivity of the polymer, $A = l\mathring{u}w$ corresponds to the electrode area with length l and width w, and h indicates the

thickness of the dielectric (as shown in Figure 4.1). The differentiation process yields the desired relative change in capacitance.

$$\frac{\Delta C}{C_0} = \left(\frac{\Delta l}{l_0} + \frac{\Delta w}{w_0} + \frac{\Delta h}{h_0}\right) = \varepsilon_x + \varepsilon_y - \varepsilon_z \tag{4.2}$$

Considering the plane-stress condition and applying Hooke's Law, the change in capacitance (ΔC) as a function of surface strain can be expressed as follows:

$$\frac{\Delta C}{C_0} = \frac{1}{1-\nu_0}\left(\varepsilon_x + \varepsilon_y\right) = \lambda_0\left(\varepsilon_x + \varepsilon_y\right) \tag{4.3}$$

In the presence of surface corrugation on the dielectric layer, there is a modification in the in-plane stiffness, resulting in an orthotropic transverse Poisson's ratio denoted as $\nu_{xy} = -\frac{-\epsilon_y}{\epsilon_x}$. Consequently, Equation 4.3 can be rewritten as follows:

$$\frac{\Delta C}{C_0} = \frac{1-\nu_{xy}}{1-\nu}\varepsilon_x = \lambda\varepsilon_x \tag{4.4}$$

Equation 4.4 can be tailored to suit a composite configuration in which the transverse Poisson's ratio is altered as a result of the composite effect with the materials to which the sensor is adhered. In this composite setup, the modified equation for the relative change in capacitance can be expressed as follows:

$$\nu_{xy,c} = \frac{a\nu_{xy} + b\nu_m}{a+b} \tag{4.5}$$

Considering the composite effect with the monitored material, where ν_m is the Poisson's ratio of the monitored material, and a and b are weight coefficients representing the contribution of each material, with $a+b=1$, depending on the level of adhesion and material stiffnesses. The resulting gauge factor under the composite effect can be expressed as follows:

$$\lambda = \frac{1-\nu_{xy,c}}{1-\nu} \tag{4.6}$$

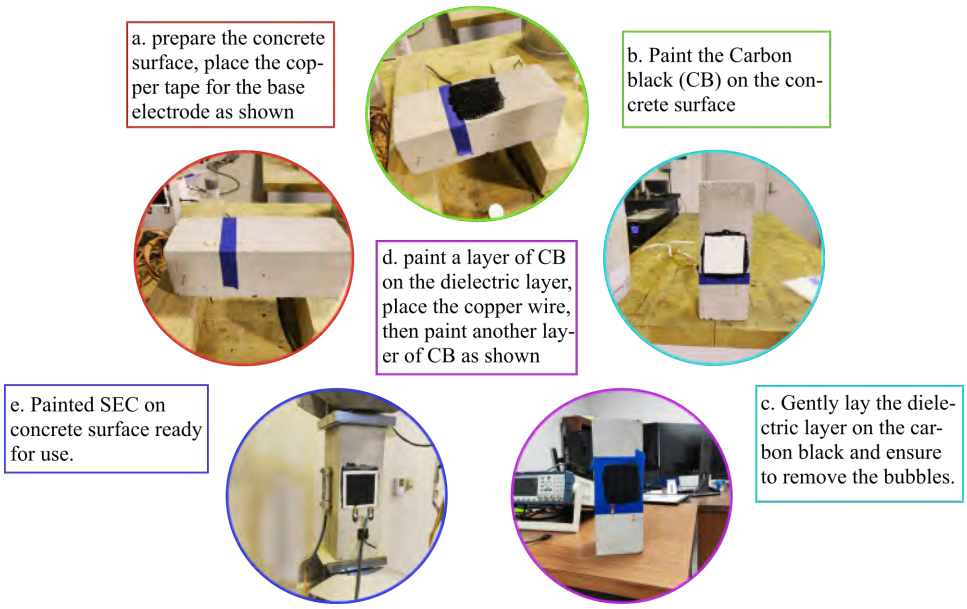

Figure 4.2 extended SEC where (a) shows the dry and ready-for-use sensor, and; (b) the schematic of the layers making up the extended sensor.

4.3 Methodology

This section describes in details the process of painting the SEC directly on the monitored surface using the carbon black solution. The experimental setup and testing procedure use to evaluate the SEC performance are also discussed.

4.3.1 Adhesion process

Surface preparation is critical in ensuring strong adhesion between soft elastomeric capacitors and monitored surfaces. The concrete surface is mechanically abraded using sandpaper. Abrasion roughens the surface, enhancing the mechanical interlocking between the elastomeric material and the concrete substrate. A similar abrasion technique can be used on metal surfaces. Initial cleaning involves removing dust, dirt, and loose particles using compressed air or a brush for concrete surfaces. A suitable detergent solution is then applied to clean any oil, grease, or organic residues on the surface. The concrete surface is thoroughly rinsed with water and allowed to dry completely before proceeding to adhered the cSEC.

In the direct painting procedure, the electrode (carbon black solution) of the SEC is

directly applied to the cleaned and prepared surface using various techniques, including brushing or spraying. First, a copper wire is placed on the concrete surface and held with a tape, Figure 4.2(a). In this work, the CB solution is gently brushed unto the surface of the concrete with enough surface area to accommodate the dielectric layer as shown in Figure 4.2(b) The dielectric layer (elastomeric material) is then laid on the painted CB solution and allowed to dry for about six hours, Figure 4.2(c). The second electrode layer is then painted onto the dielectric layer while also attaching the connections copper wire, as shown in the Figure 4.2(d). Finally, the tapes on the SEC is then removed after allowing the SEC to dry for at least 12 hours. Figure 4.2(d) shows a ready-to-test concrete sample with attached painted cSEC under compression loading by the dynamic testing system.

Epoxy bonding involves using off-the-shelf bi-component epoxy (JB Weld) to attach the cSEC to the prepared surface. A thin layer of the epoxy adhesive is applied to the surface, and then the sensor is gently laid on top, ensuring to remove bubble layer of adhesive under the SEC. The choice of epoxy adhesive is crucial for achieving strong and durable bonding between the elastomeric material and the monitored surface. High-performance epoxy adhesives with good bonding properties, low shrinkage, and excellent environmental resistance are preferred.

4.3.2 Test setup

The experimental techniques used to investigate the sensor performance are described in this section. First, we evaluate the painted cSEC's sensing properties after it has been adhered with carbon black. The tests to evaluate the sensing capacities of the CB-painted cSEC and epoxy-adhered cSEC at different thicknesses are then discussed.

Cantilever plate

The CB-painted cSEC's sensing capabilities, including strain sensitivity, signal linearity, and resolution, were assessed using a homogeneous material (steel cantilever plate) bent under tension. Figure 4.3(d) depicts the experiment's general layout. A steel plate with dimensions of 16 $\times$ 4 $\times$ 0.125 inches was tightly clamped using two grips of the dynamic

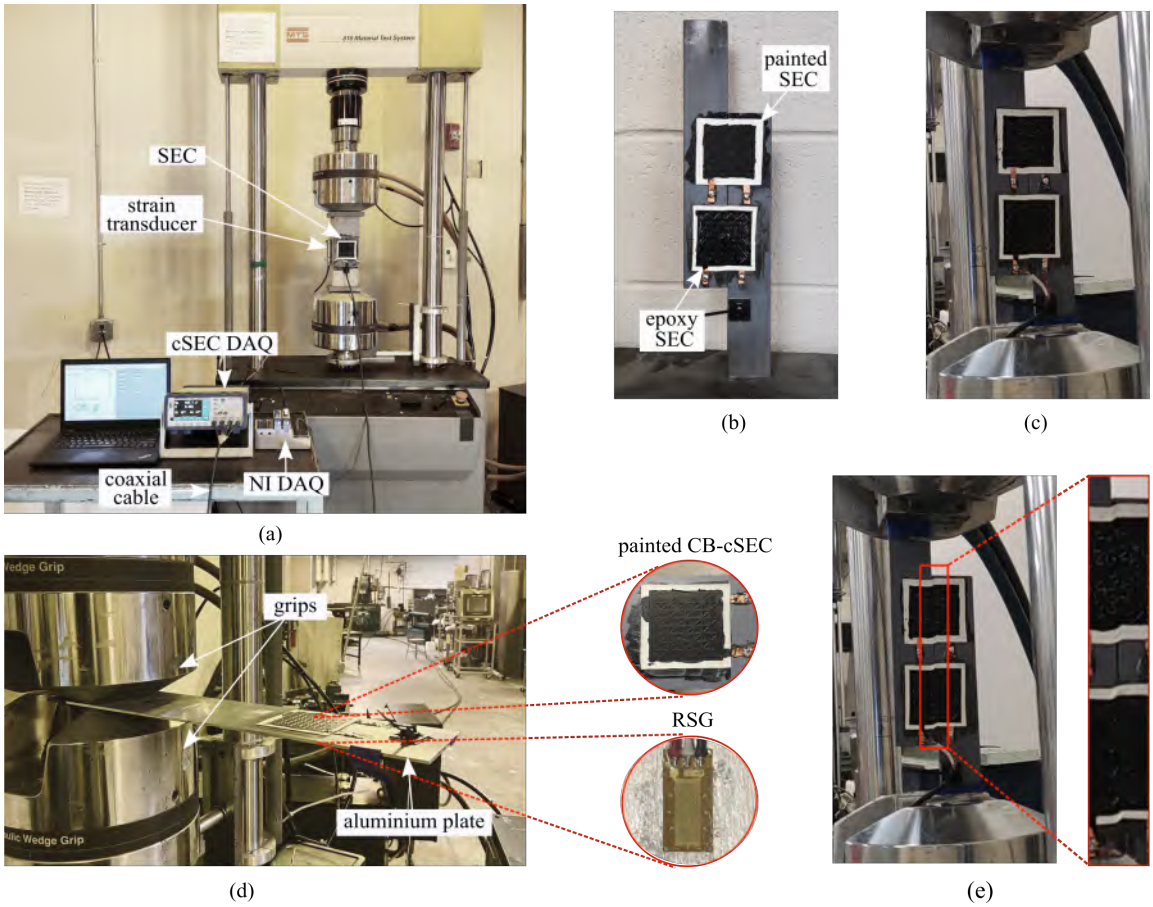

Figure 4.3 Concrete samples where (a) shows three sample od thicknesses of 3, $2_{1/2}$, 2 inch; (b) a concrete sample with the SEC attached using an off-the-shelf bicomponent epoxy (JB Weld), and (c) a concrete sample with SEC directly painted on its surface.

testing system. A suitable bonding area for the sensor was created on the surface of the steel plate by sanding it with sandpaper before being cleaned with acetone to remove other impurities. The bonding process of the CB-painted cSEC on steel is the same as described on concrete; however, the surface of the steel was coated with a non-conductive primer before the adhesion of the CB-painted cSEC. The CB-painted cSEC was allowed to dry for at least 12 hours before any test. For benchmarking purposes, a resistive strain gauge (RSG) with a nominal resistance of 350 ohms by Micro-Measurements was attached on the opposite side of the plate with M-bond 200 adhesive kit as shown in the inset of Figure 4.3(d).

A quasi-static test was carried out by gently applying upward and downward pressure to the free end of the cantilever plate to create tensile and compressive bending strains. Data from the CB-painted cSECs were gathered using a BK Precision 891 LCR meter,

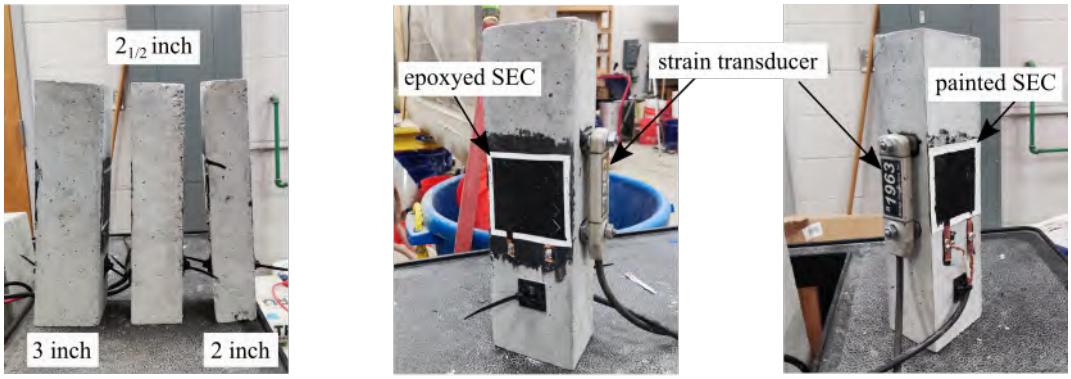

(a) (b) (c)

Figure 4.4 Concrete samples where (a) shows three sample od thicknesses of 3, $2_{1/2}$, 2 inch; (b) a concrete sample with the SEC attached using an off-the-shelf bicomponent epoxy (JB Weld), and (c) a concrete sample with SEC directly painted on its surface.

referred to as cSEC DAQ in Figure **??**(a), at a sampling rate of 45 samples per second (S/s). Active shielded coaxial cables were employed to connect the cSECs to the DAQs to prevent parasitic noise. A 24-bit, 350-ohm, 3/4-bridge analog input module from National Instruments (NI-9236) was used to record data from the RSG at a sampling rate of 1000 S/s. No signal filtering was used, and both DAQs were run simultaneously within the LabVIEW environment.

Sensor performance on concrete

The performance of the CB-painted cSEC on unreinforced concrete samples was evaluated using compressive tests on concrete samples of three different sizes, 12 × 3 × 3 inch, 12 × 3 × 2.5 inch and 12 × 3 × 2 inch. Results from the CB-painted cSECs on the concrete surface were compared to those of a cSEC adhered using an epoxy ("epoxied SEBS-cSEC") and a resistance strain gauge (RSG), which was also adhered to each of the concrete samples as shown in Figure 4.4(b) and (c). The SEBS-cSECs used in this test were fabricated by following the procedure reported in [57], and their initial capacitance was kept between 220 and 260 pF under 1 kHz measuring frequency by the BK precision LCR meter. A bi-component epoxy (JB Weld) is used to adhere the epoxy-SEBScSEC. Tests were carried out on the dynamic testing system by MTS to load the concrete sample compressively. A low cycle load of the same amplitude at 0.05 Hz was applied to each concrete sample to monitor

the SEC signal on concrete of different sizes. The tests were conducted over three times to investigate the repeatability of results. Data were collected using the same setup as the CB painted-cSEC and epoxy-adhered cSEC. At the same time, the signal from the RSG was recorded using the analog input module National Instruments NI-9237. (Figure 4.3(a)).

Investigations on the expected thickness of the cSEC layer are then carried out using a concrete sample of dimension $12 \times 4 \times 4$ inches. The tests were done for the epoxyed cSEC and CB-painted cSECs. cSECs of thicknesses 0.28, 0.36, 0.48, and 0.56 mm were accessed for the epoxyed test, while cSEC dielectric layer of thicknesses 0.23, 0.37, 0.40, 0.46, and 0.56 mm were tested for CB-painted cSEC. All tests used an RSG signal as a reference for strain comparison on the concrete sample.

Shear test

This test seeks to investigate the behavior of the CB-painted SEC in situations of shearing or crack, which could potentially lead to discontinuity of the painted electrodes, especially if in a significant shear occurrence. However, the mechanical properties of the painted CB are similar to the dielectric layer, so it is expected to allow the painted electrode layer to deform alongside the monitored surface without discontinuity. Figure 4.3(b) shows the angle bar used for the investigation with CB-painted cSEC at the top and epoxy-bonded cSEC below. Two angle bar were align together such that one could be slide on top the other which could generate a shear deformation on the attached sensor. Figure 4.3(c) relates the dynamic loading of the angle bar with the MTS machine with Figure 4.3(e) showing the shear in the angle bar with the inset showing slight deformation in the attached SECs due to shear.

4.4 Results and Analysis

This section presents and discusses the experimental results. First, the electromechanical behavior of a single painted CB-cSEC is characterized. Second, the sensing performance of the painted CB-cSEC on concrete is compared against that of an epoxied SEBS-cSEC,

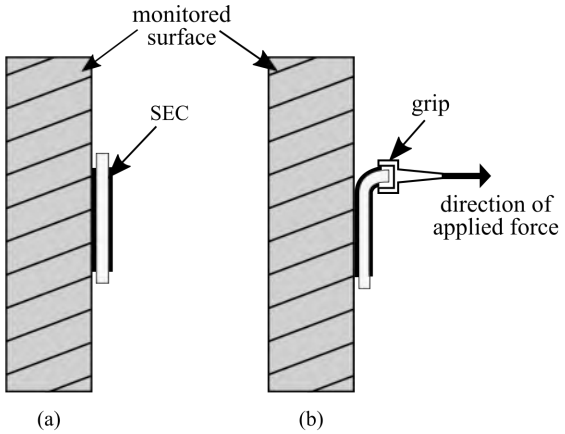

Figure 4.5 Concrete samples where (a) shows three sample od thicknesses of 3, $2_{1/2}$, 2 inch; (b) a concrete sample with the SEC attached using an off-the-shelf bicomponent epoxy (JB Weld), and (c) a concrete sample with SEC directly painted on its surface.

and the effect of direct painting is assessed. Further investigations on the dielectric layer thickness for the painted CB-cSEC were also reported.

4.4.1 Adhesion strength

The adhesion strength for the CB-painted cSEC and epoxied cSEC on concrete and metal surfaces was evaluated by subjecting the prepared sensors to controlled mechanical stress to assess their adhesion strength. Figure **??**(a) and (b) shows the process layout used to test the adhesion strength. An incremental force was applied to a slight edge layer of the SEC until it started peeling off the concrete or metal surface.

The results indicated that the adhesion strength of SECs adhered using direct painting varied significantly depending on the surface type and preparation. Concrete surfaces with roughened profiles showed superior adhesion, with an average peel force of 25 N/cm². However, on smooth concrete surfaces, the adhesion strength decreased to an average peel force of 15 N/cm². For metal surfaces, mechanically abraded metal surfaces exhibited higher adhesion strength, with an average peel force of 30 N/cmš. Conversely, the average peel force on smooth metal surfaces was reduced to 20 N/cm².

The adhesion strength for epoxied cSEC involved using the bi-component off-the-shelf (JB Weld) epoxy to bond cSEC onto concrete and metal surfaces. The sensors were subjected to the same controlled mechanical stress to evaluate their adhesion strength. The

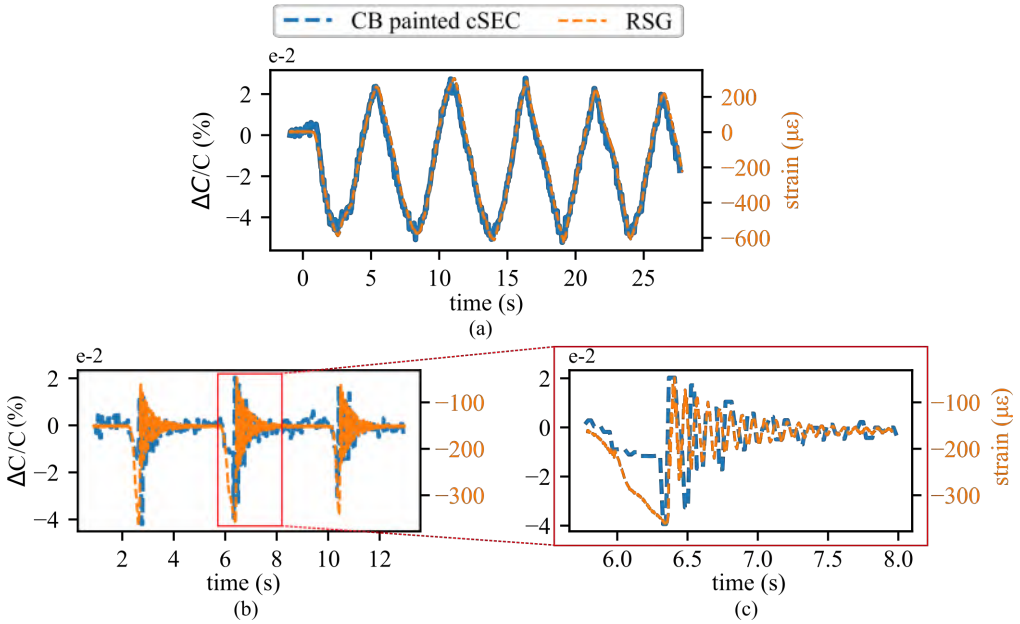

Figure 4.6 Concrete samples where (a) shows three sample od thicknesses of 3, $2_{1/2}$, 2 inch; (b) a concrete sample with the SEC attached using an off-the-shelf bicomponent epoxy (JB Weld), and (c) a concrete sample with SEC directly painted on its surface.

average peel force of epoxy-bonded sensors for concrete surfaces was consistently high at 35 N/cmš, regardless of the surface roughness. Similarly, epoxy bonding exhibited remarkable adhesion strength on metal surfaces, with an average peel force of 40 N/cmš, irrespective of the surface treatment method used.

The results showed that both adhesion methods are suitable for bonding the SEC without concerns about loss of contact between the sensor and the monitored surface.

4.4.2 Electro-Mechanical Behavior

Figure 4.6(a) presents a time series plot of the raw data measured from a single CB-painted cSEC, showing the relative change in capacitance $\Delta\ C/C_0$ and the applied strain measured from the RSG. A significantly close match between the CB-painted cSEC and RSG signals can be observed. The resulting root mean square error (RMSE) and mean absolute percentage error (MAPE) of the fit are 5.98% and 6.08%, respectively. Figure 4.6(b) plots the relative change in capacitance $\Delta\ C/C_0$ from the SEC versus the applied strain from the RSG under free vibration, which is a more dynamic test for the SEC—under the free

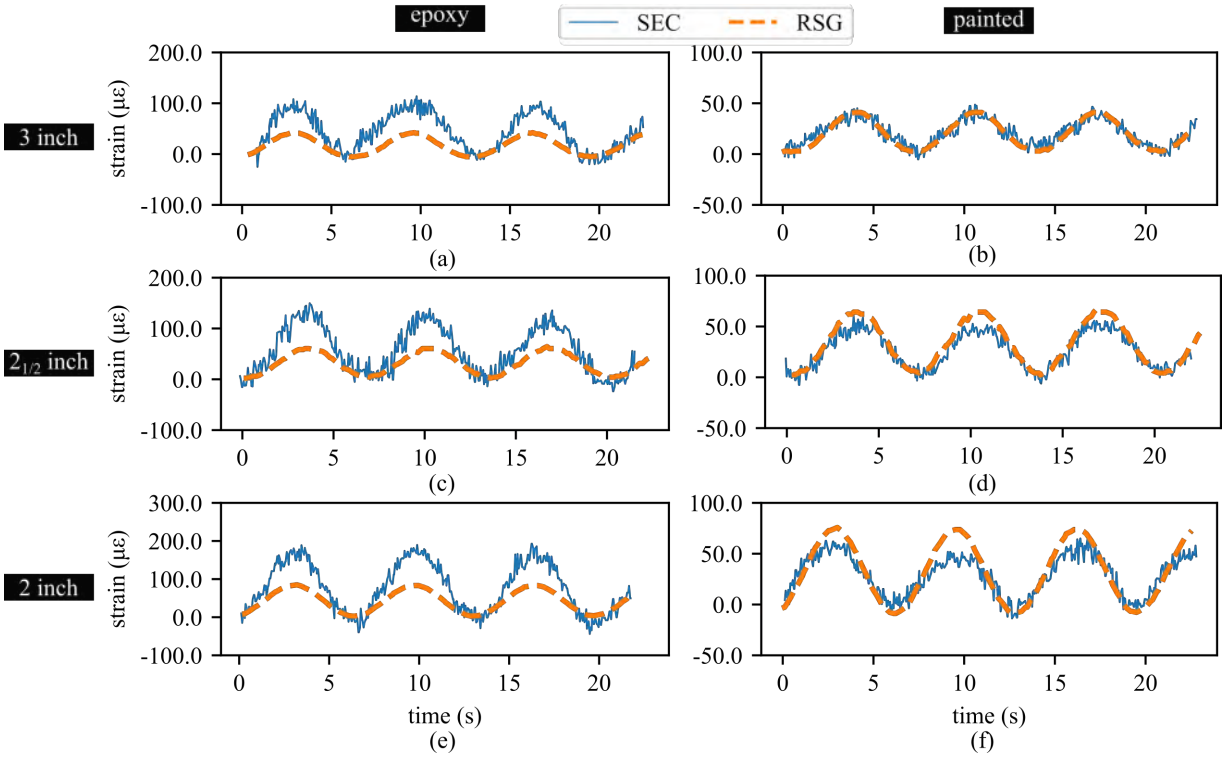

Figure 4.7 Strain data from concrete samples of different thickness showing strain on concrete of (a) 3 inch thick and epoxyed SEC; (b) 3 inch thick and painted SEC; (c) $2_{1/2}$ thick and epoxyed SEC; (d) $2_{1/2}$ thick and painted SEC; (e) 2 inch thick and epoxyed SEC, and; (f) 2 inch thick and painted SEC.

vibration test, the CB-painted SEC represented a free vibration of the plate well. The results observed, even though not as smooth as that from the RSG, the initiation and end phase of the vibration were appreciable, as seen in Figure 4.6(c). This data shows that the sensitivity of the CB-painted SEC is good as it measures the induced vibration on the plate with an accuracy of [].

4.4.3 Strain test on concrete

The CB-painted and epoxy-adhered cSECs were used to test for the strain on concrete samples as described in section 4.3. Three concrete samples of different dimensions were used for the initial test of the sensors for strain. Samples of dimension 12 × 3 × 3 inch, 12 × 3 × $2_{1/2}$ inch and 12 × 3 × 2 inch were used. as shown in Figure 4.4(a). Each sample was subjected to the same compressive loading from the dynamic testing system by the MTS of the model. Figure 4.4(b) and (c) show a concrete sample with an SEC sensor

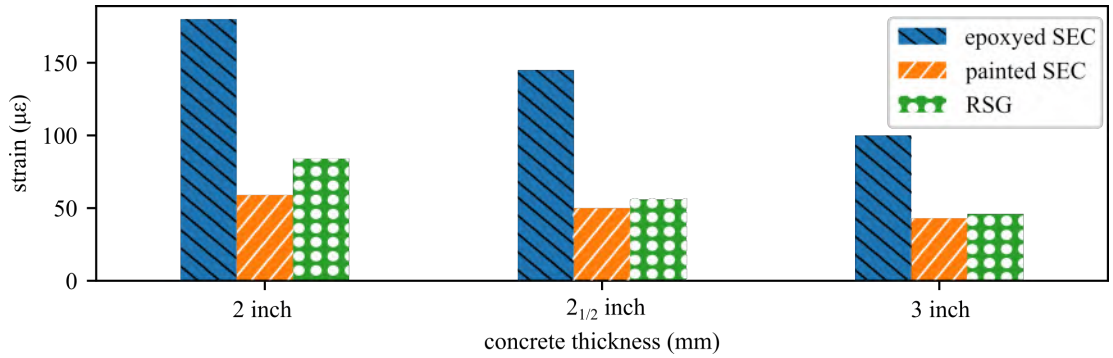

Figure 4.8 Barplot showing strain from the SEC adhered with epoxy and direct painting and resistant strain gauge on concrete of thicknesses 3, $2_{1/2}$, 2 inch.

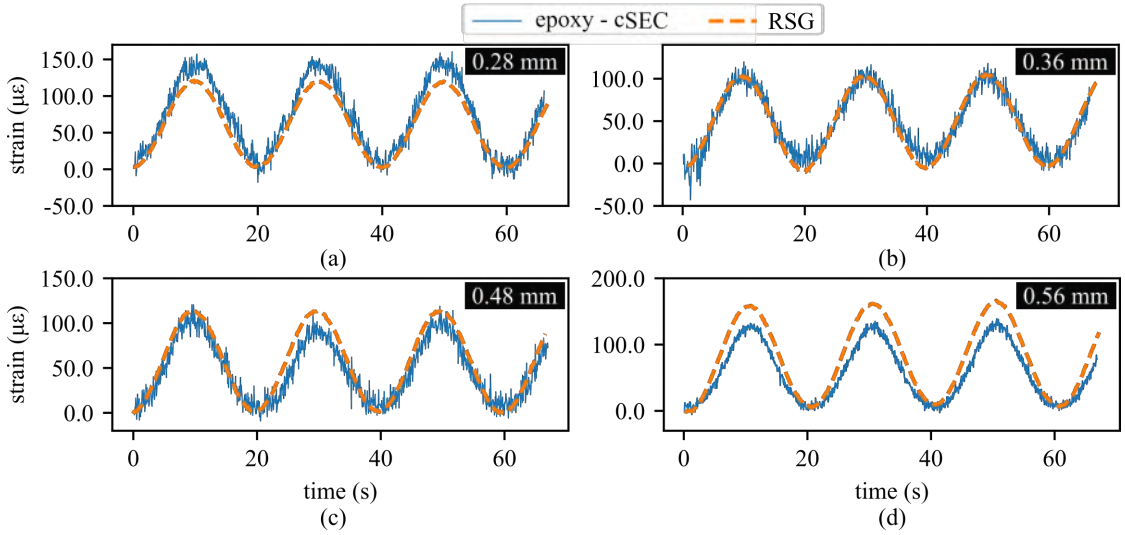

Figure 4.9 extended SEC where (a) shows the dry and ready-for-use sensor, and; (b) the schematic of the layers making up the extended sensor.

attached on the surface with epoxy and by direct painting, respectively, alongside a BDI strain transducer as a reference sensor.

The strain results reported in Figure 4.7 are compressive due to the compressive load applied to the concrete samples. The sensor's response to the same load at varied thicknesses of the concrete sample changes as the concrete thickness varies. For the 3-inch thick concrete sample shown in figure 4.7(a) and (b), the epoxy-adhered SEC displayed a higher response to load compared to the directly painted SEC. The observed strain response of the sensor is also repeatedly seen in the $2_1/2$ and 2-inch concrete samples in Figure4.7(c), (d), (e), and (f). Though the epoxy-adhered SEC has a layer of adhesive between the sensor and the concrete surface, it reported a higher strain than the SEC on direct contact with the

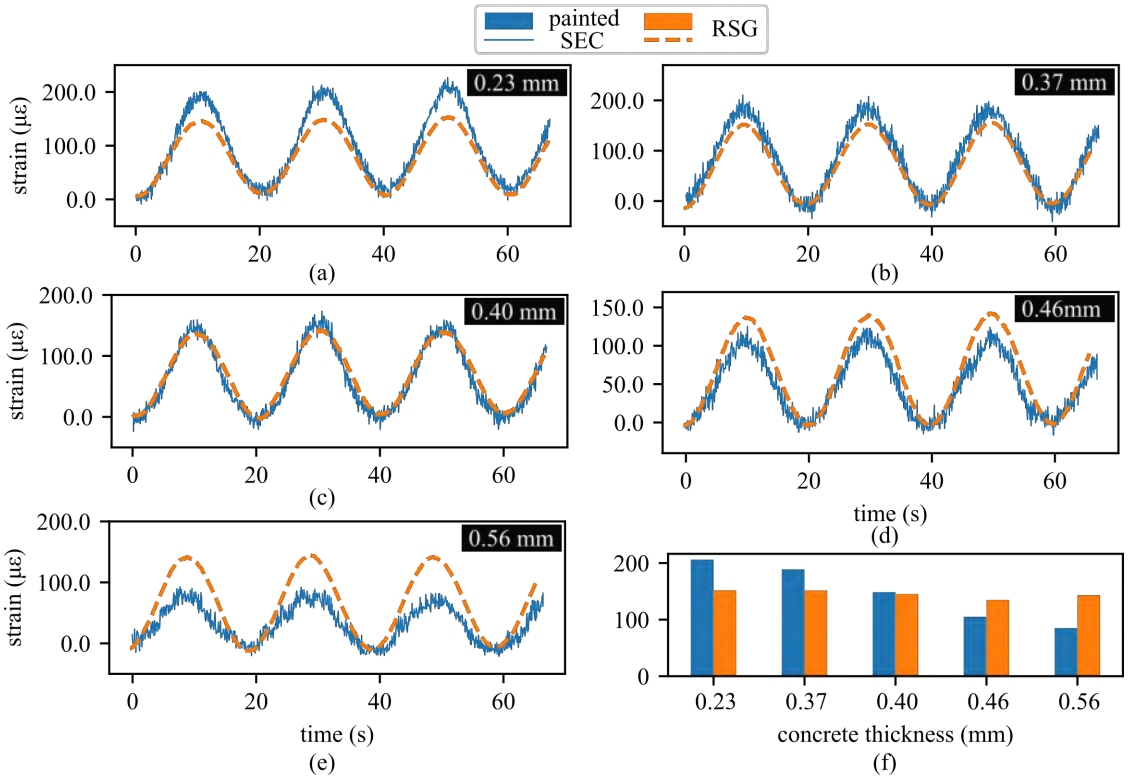

Figure 4.10 extended SEC where (a) shows the dry and ready-for-use sensor, and; (b) the schematic of the layers making up the extended sensor.

concrete surface. Figure 4.8 shows how the two adhesion methods relate with the reference strain transducer, and in all three thicknesses of concrete observed, the direct painted SEC gives a closer strain value to the reference strain. Also, strain measure commensurate with the thickness of concrete being measured with the thicker concrete sample reporting less strain.

4.4.4 Effect of sensor thickness on measured strain

In light of the SEC's response in section 4.4.3, the cSEC response to load is then tested on a concrete of thickness 12 × 4 × 4-inch using cSEC with different thickness. The test varied the overall thickness of the SEC for the epoxy-adhered cSEC and the dielectric layer's thickness for the CB-painted cSEC.

In Figure 4.9(a) to (d), four compressive strain test was carried out using epoxy-cSEC of thicknesses 0.28, 0.36, 0.48, and 0.56 mm, and strain results were compared to the reference

strain transducer earlier mentioned. The figures report that thinner SEC improves the sensor sensitivity; however, it does not equate to accuracy as observed in the 0.28 mm thick SEC, where the signal is well represented but overestimated. In contrast, the thicker the SEC, the less sensitive it is to mechanical loading, as depicted in Figure 4.9(d) of 0.56 mm thickness. A better-aligned strain data is seen in figure 4.9(c) where SEC of thickness 0.36 mm is used, and further testing with epoxy-adhered SEC should be of this thickness.

The CB-painted cSEC is then tested on the exact dimension of the concrete sample, where the thickness of the dielectric layer is varied. Thicknesses similar to the epoxy-adhered cSECs were used, which are 0.23, 0.37, 0.40, 0.46, and 0.56 mm. Figure 4.10(a) to (e) shows the strain measured by each of the CB-painted cSECs in increasing order of thickness. A comparable signal to that of the epoxy-adhered cSEC is depicted as the thickness of the SEC increases. It can also be said that the sensitivity of the CB-painted cSEC decreases as the dielectric layer increases. Figure 4.10(f) shows the strain measured by the CB-painted cSEC and RSG as the thickness increases. A dielectric layer of thickness 0.40 mm is observed to transducer a closer strain value to the reference strain on the concrete sample.

4.4.5 Performance under shear of monitored surface

Two angle bars of steel material were used to test the CB-painted and epoxy cSEC when monitoring a shear/crack-related process. Figure 4.3(b) shows the angle bar joined with a sliding hinge, with the CB-painted SEC at the top and the epoxy-adhered below the CB-painted SEC. The test operation is displayed in Figure 4.3(c) and (e) where Figure 4.3(c) is the rest position of the angle bar with no shear, and Figure 4.3(e) shows a displacement in position due to dynamic loading of the angle bar resulting in shear deformation on the SECs attached as shown in the inset of figure 4.3(c).

At the position of rest, an excellent static signal (low noise) is recorded from both CB-painted and epoxy-adhered SEC as shown in Figure 4.11(a) and Figure 4.11(b) respectively, which is expected for a good SEC sensor. Responses to incremental displacement by the two SECs are shown in Figure 4.11(c) for CB-painted SEC and Figure 4.11(d) for epoxy-adhered SEC. Direct observations of the two responses indicate that the epoxy SEC responds

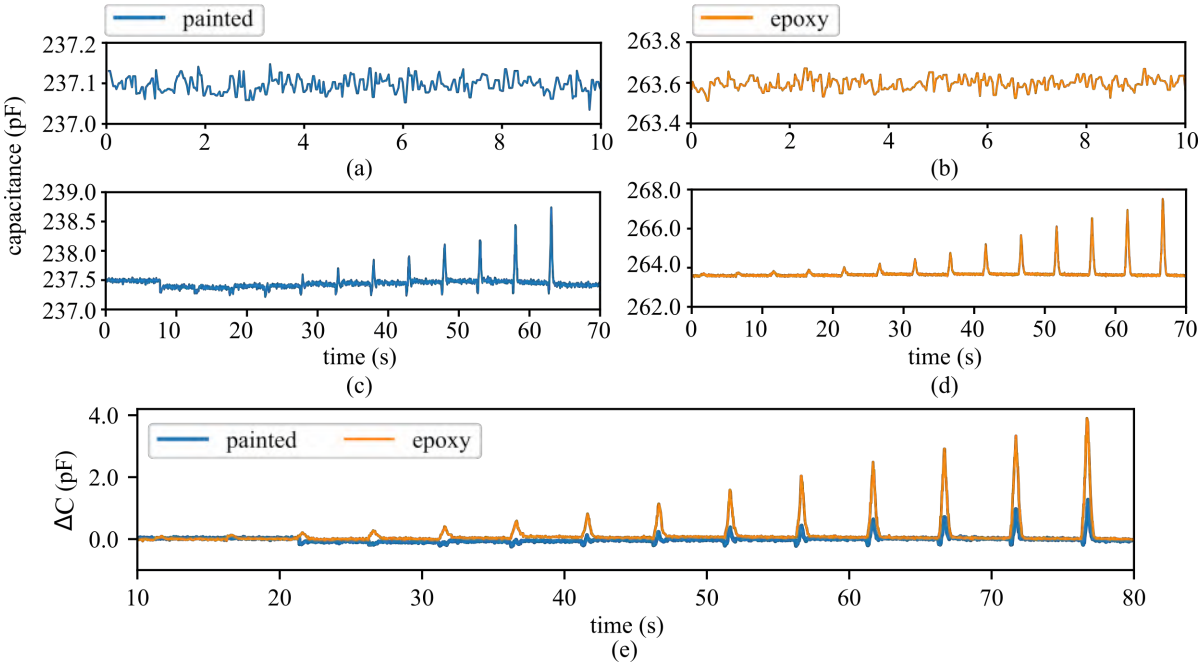

Figure 4.11 extended SEC where (a) shows the dry and ready-for-use sensor, and; (b) the schematic of the layers making up the extended sensor.

better to capacitance change. The first four starting displacement monitored by the CB-painted SEC is poor as the signal is reversed and not distinct; however, as the displacement introduced increased, a much more precise and better signal is monitored. The initial reversed signal may have occurred due to discontinuity in the conductive layer (electrode) painted on the surface of the angle bar.

Figure 4.11(e) presents a side-by-side comparison of the two sensors and shows that the sensitivity of the epoxy-adhered SEC is higher than the CB-painted SEC as it recorded a higher capacitance change with equal displacement.

4.5 Conclusion

This paper presented a carbon black-painted corrugated soft elastomeric capacitor (CB-painted cSEC) that can be directly painted onto a monitored surface. The painted cSEC was achieved using CB paint to adhere the SEC to the monitored surface. The dielectric layer is fabricated using the styrene-ethylene-butadiene-styrene (SEBS) block co-polymer and TiO_2, while the electrode layer is a solution mixture of SEBS and CB. The adhesion

strength of the two bonding approaches used was studied and observed to be about 25 N/cm^2 on the concrete surface and 30 N/cm^2 on metals for the CB-painted cSEC, and about 35 N/cm^2 on the concrete surface and 40 N/cm^2 on metals for the epoxied-cSEC. Its sensing properties in terms of linearity and resolution were characterized through a quasi-static bending test and free vibration of a cantilever beam. This resolution compared well with the epoxied SEBS-cSEC reported in previous work. The CB-painted and epoxied cSEC are used to monitor strain on concrete samples of different sizes; both cSEC had a similar response as higher strain value was observed in the smaller concrete sample compared to the bigger dimension. The result observed showed... Further investigations on concrete strain monitoring using different cSEC thicknesses were carried out, indicating a best-fit thickness of 0.36 mm for the epoxied cSEC and 0.40 mm dielectric layer thickness for the CB-painted cSEC.

Acknowledgments

The authors gratefully acknowledge the financial support of the Departments of Transportation of Iowa, Kansas, South Carolina, and North Carolina, through the Transportation Pooled Fund Study TPF-5(449).

Declaration of competing interest

The authors declare no conflict of interests

Chapter 5

Conclusion

Soft elastomeric capacitors (SECs) have emerged as a pivotal tool in the realm of structural health monitoring, environmental sensing, and human-machine interaction. Their versatility and potential applications span from monitoring concrete infrastructure to wearable electronics. However, their efficiency and reliability are contingent upon their adhesion to various surfaces, particularly concrete and metals.

In the quest to optimize the adhesion of SECs, two primary methods were explored: direct painting with carbon black (CB) and epoxy bonding. The direct painting method, which involves applying the elastomeric material directly onto the surface, offers simplicity and cost-effectiveness. However, concerns about its long-term stability in demanding environmental conditions arise. On the other hand, epoxy bonding, which uses specialized adhesives, provides exceptional adhesion strength, making it suitable for harsh environments and extended monitoring applications.

The study on the SEC with an extra layer of SEBS (styrene-ethylene-butadiene-styrene) aimed to minimize the capacitive coupling between the SEC and concrete. This was crucial as capacitive coupling often leads to overestimated measurements. The findings revealed that the extended SEC, when compared to the traditional SEC, provided more accurate strain measurements, especially when validated against digital image correlation.

Furthermore, a novel approach was introduced with the carbon black-painted corrugated soft elastomeric capacitor (CB-painted cSEC) that can be directly painted onto a monitored surface. This method showcased promising adhesion strengths on both concrete and metal surfaces. The painted cSEC utilized CB paint for adhesion, with the dielectric layer crafted from SEBS block co-polymer and TiO2. The adhesion strength of the CB-painted cSEC was

found to be about $25N/cm^2$ on concrete and $30N/cm^2$ on metals, while the epoxied-cSEC exhibited slightly higher strengths.

In conclusion, the advancements in the field of soft sensors, particularly SECs, are promising for a wide range of applications. The research underscores the importance of optimizing adhesion methods to ensure the sensors' longevity and accuracy. As the world moves towards more integrated and smart systems, the role of such sensors, especially in structural health monitoring, will become increasingly pivotal. Future research should continue to refine these adhesion techniques and explore the potential of SECs in diverse environments and applications.

Bibliography

[1] Qingfei Gao, Yu Wang, Jun Li, Kejian Sheng, and Chenguang Liu. An enhanced percolation method for automatic detection of cracks in concrete bridges. *Advances in Civil Engineering*, 2020:1–23, 2020.

[2] Achim Hering. bridge, 13 July 2012. Retrieved from https://commons.wikimedia.org/wiki/File:Qew_bruecke_nf_beton_kaputt_32_von_46.jpg.

[3] Cristian V. Strain gauge, 5 December 2017. Figure modified and was retrieved from https://commons.wikimedia.org/wiki/File:Strain_gauge_-.jpg.

[4] Dr. Rüdiger Paschotta. Fiber bragg gratings. Encyclopedia of Laser Physics and Technology, 1. edition, October 2008. Retrieved from https://www.rp-photonics.com/fiber_bragg_gratings.html.

[5] Passive Components. Linear variable differential transformers lvdts explained, 2023. Retrieved from https://passive-components.eu/linear-variable-differential-transformers-lvdts-explained/.

[6] Mohammed Almarwae. Structural failure of buildings: Issues and challenges. *World Scientific News*, (66):97–108, 2017.

[7] International Association for Bridge, Structural Engineering. Bangladesh Group, and Doboku Gakkai. Bridge collapses around the world: Causes and mechanisms. page 651.

[8] Satish Chandra. Bridge failure and consequences. volume 7. JETIR, 2020.

[9] Gangbing Song, Chuji Wang, and Bo Wang. Structural health monitoring (shm) of civil structures. *Applied Sciences (Switzerland)*, 7, 8 2017.

[10] Ekin Ozer and Maria Q. Feng. Structural health monitoring. pages 345–367. Elsevier, 2020.

[11] Shukla Alokita, Verma Rahul, Kandasamy Jayakrishna, VR Kar, M Rajesh, S Thirumalini, and M Manikandan. Recent advances and trends in struc-

tural health monitoring. In *Structural health monitoring of biocomposites, fibre-reinforced composites and hybrid composites*, pages 53–73. Elsevier, 2019.

[12] Piotr Omenzetter, Ufuk Yazgan, Serdar Soyoz, and Maria Pina Limongelli. Quantifying the value of shm for emergency management of bridges at-risk from seismic damage. In *Joint COST Actions TU1402 & TU1406 and IABSE WC1 Workshop: Quantifying the Value of Structural Health Monitoring for the Reliable Bridge Management*, pages 4–5, 2017.

[13] Simon Laflamme, Hussam S Saleem, Bharath K Vasan, Randall L Geiger, Degang Chen, Michael R Kessler, and Krishna Rajan. Soft elastomeric capacitor network for strain sensing over large surfaces. *IEEE/ASME Transactions on Mechatronics*, 18(6):1647–1654, 2013.

[14] Han Liu, Simon Laflamme, Eric M Zellner, Adrien Aertsens, Sarah A Bentil, Iris V Rivero, and Thomas W Secord. Soft elastomeric capacitor for strain and stress monitoring on sutured skin tissues. *ACS sensors*, 6(10):3706–3714, 2021.

[15] Sari Kharroub, Simon Laflamme, Chunhui Song, Daji Qiao, Brent Phares, and Jian Li. Smart sensing skin for detection and localization of fatigue cracks. *Smart Materials and Structures*, 24(6):065004, 2015.

[16] Sdiq Anwar Taher, Jian Li, Jong-Hyun Jeong, Simon Laflamme, Hongki Jo, Caroline Bennett, William N Collins, and Austin RJ Downey. Structural health monitoring of fatigue cracks for steel bridges with wireless large-area strain sensors. *Sensors*, 22(14):5076, 2022.

[17] Austin RJ Downey, Jin Yan, Eric M Zellner, Karl H Kraus, Iris V Rivero, and Simon Laflamme. Use of flexible sensor to characterize biomechanics of canine skin. *BMC veterinary research*, 15(1):1–10, 2019.

[18] Ozgur Atalay. Textile-based, interdigital, capacitive, soft-strain sensor for wearable applications. *Materials*, 11(5):768, 2018.

[19] Sari Kharroub, Simon Laflamme, Chunhui Song, Daji Qiao, Brent Phares, and Jian Li. Smart sensing skin for detection and localization of fatigue cracks. *Smart Materials and Structures*, 24(6):065004, 2015.

[20] Branko Glišić, David Hubbell, Dorotea Hoeg Sigurdardottir, and Yao Yao. Damage detection and characterization using long-gauge and distributed fiber optic sensors. *Optical Engineering*, 52:087101, 8 2013.

[21] Sihai Wen and D. D.L. Chung. Electromagnetic interference shielding reaching 70 db in steel fiber cement. *Cement and Concrete Research*, 34:329–332, 2 2004.

[22] Emmanuel Ogunniyi, Alexander Vereen, Austin Downey, Simon Laflamme, Jian Li, Caroline R Bennett, William Collins, Hongki Jo, Alexander Henderson, and Paul Ziehl. Investigation of electrically isolated capacitive sensing skins on concrete to reduce structure/sensor capacitive coupling. *Measurement Science and Technology*, 2023.

[23] Emmanuel A Ogunniyi, Han Liu, Austin RJ Downey, Simon Laflamme, Jian Li, Caroline Bennett, William Collins, Hongki Jo, and Paul Ziehl. Soft elastomeric capacitors with an extended polymer matrix for strain sensing on concrete. In *Sensors and Smart Structures Technologies for Civil, Mechanical, and Aerospace Systems 2023*, volume 12486, pages 262–270. SPIE, 2023.

[24] Emmanuel Ogunniyi, Alexander Vareen, Austin RJ Downey, Simon Laflamme, Jian Li, Caroline Bennett, William Collins, Hongki Jo, Alexander Henderson, and Paul Ziehl. Investigation of electrically isolated capacitive sensing skins on concrete to reduce structure/sensor capacitive coupling. *Measurement Science and Technology*, 34(5):055113, 2023.

[25] Maxwell James Davis and A McGregor. Assessing adhesive bond failures: mixed-mode bond failures explained. In *ISASI Australian Safety Seminar, Canberra*, pages 4–6, 2010.

[26] S. T. Tung, Y. Yao, and B. Glisic. Sensing sheet: The sensitivity of thin-film full-bridge strain sensors for crack detection and characterization. *Measurement Science and Technology*, 25, 2014.

[27] Yao Yao and Branko Glisic. Sensing sheets: Optimal arrangement of dense array of sensors for an improved probability of damage detection. *Structural Health Monitoring*, 14:513–531, 9 2015.

[28] Daniele Zonta, Andrea Chiappini, Alessandro Chiasera, Maurizio Ferrari, Matteo Pozzi, Lorenzo Battisti, and Matteo Benedetti. Photonic crystals for monitoring fatigue phenomena in steel structures. volume 7292, page 729215. SPIE, 3 2009.

[29] Kenneth J. Loh, Tsung Chin Hou, Jerome P. Lynch, and Nicholas A. Kotov. Carbon nanotube sensing skins for spatial strain and impact damage identification. *Journal of Nondestructive Evaluation*, 28:9–25, 2009.

[30] Sukhoon Pyo, Kenneth J Loh, Tsung-Chin Hou, Erik Jarva, Jerome P Lynch, et al. A wireless impedance analyzer for automated tomographic mapping of a nanoengineered sensing skin. *Smart Structures and Systems*, 8(1):139–155, 2011.

[31] Paul A Withey, Venkata Srivishnu M Vemuru, Sergei M Bachilo, Satish Nagarajaiah, and R Bruce Weisman. Strain paint: Noncontact strain measurement using single-walled carbon nanotube composite coatings. *Nano letters*, 12(7):3497–3500, 2012.

[32] Tsung Chin Hou and Jerome P. Lynch. Electrical impedance tomographic methods for sensing strain fields and crack damage in cementitious structures. *Journal of Intelligent Material Systems and Structures*, 20:1363–1379, 7 2009.

[33] Austin Downey, Antonella D'Alessandro, Micah Baquera, Enrique García-Macías, Daniel Rolfes, Filippo Ubertini, Simon Laflamme, and Rafael Castro-Triguero. Damage detection, localization and quantification in conductive smart concrete structures using a resistor mesh model. 148:924–935.

[34] Mohammadkazem Sadoughi, Austin Downey, Jin Yan, Chao Hu, and Simon Laflamme. Reconstruction of unidirectional strain maps via iterative signal fusion for mesoscale structures monitored by a sensing skin. 112:401–416.

[35] Simon Laflamme, Hussam S. Saleem, Bharath K. Vasan, Randall L. Geiger, Degang Chen, Michael R. Kessler, and Krishna Rajan. Soft elastomeric capacitor network for strain sensing over large surfaces. *IEEE/ASME Transactions on Mechatronics*, 18:1647–1654, 2013.

[36] Xiangxiong Kong, Jian Li, Caroline Bennett, William Collins, Simon Laflamme, and Hongki Jo. Thin-film sensor for fatigue crack sensing and monitoring in steel bridges under varying crack propagation rates and random traffic loads. *Journal of Aerospace Engineering*, 32(1):04018116, 2019.

[37] Xiangxiong Kong, Jian Li, Caroline Bennett, William Collins, Simon Laflamme, and Hongki Jo. Thin-film sensor for fatigue crack sensing and monitoring in steel bridges under varying crack propagation rates and random traffic loads. 32(1):04018116.

[38] Jin Yan, Austin Downey, Alessandro Cancelli, Simon Laflamme, An Chen, Jian Li, and Filippo Ubertini. Concrete crack detection and monitoring using a capacitive dense sensor array. *Sensors (Switzerland)*, 19, 4 2019.

[39] Austin R. J. Downey, Antonella D'Alessandro, Filippo Ubertini, and Simon Laflamme. Crack detection in rc structural components using a collaborative data fusion approach based on smart concrete and large-area sensors. page 123. SPIE-Intl Soc Optical Eng, 3 2018.

[40] Simon Laflamme, Filippo Ubertini, Hussam Saleem, Antonella D'Alessandro, Austin Downey, Halil Ceylan, and Annibale Luigi Materazzi. Dynamic characterization of a soft elastomeric capacitor for structural health monitoring. *Journal of Structural Engineering*, 141:04014186, 8 2015.

[41] Austin Downey, Anna Laura Pisello, Elena Fortunati, Claudia Fabiani, Francesca Luzi, Luigi Torre, Filippo Ubertini, and Simon Laflamme. Durability and weatherability of a styrene-ethylene-butylene-styrene (SEBS) block copolymer-based sensing skin for civil infrastructure applications. 293:269–280.

[42] Han Liu, Simon Laflamme, Jian Li, Caroline Bennett, William Collins, Austin Downey, Paul Ziehl, and Hongki Jo. Investigation of surface textured sensing skin for fatigue crack localization and quantification. *Smart Materials and Structures*, 30, 10 2021.

[43] Micro-Measurements Vishay Precision Group. Strain gage installations for concrete structures strain gages and instruments.

[44] Siqi Ding, Sufen Dong, Ashraf Ashour, and Baoguo Han. Development of sensing concrete: Principles, properties and its applications. *Journal of Applied Physics*, 126(24):241101, 2019.

[45] DDL Chung. Self-sensing concrete: from resistance-based sensing to capacitance-based sensing. *International Journal of Smart and Nano Materials*, 12(1):1–19, 2021.

[46] D.D.L. Chung and Yulin Wang. Capacitance-based stress self-sensing in cement paste without requiring any admixture. *Cement and Concrete Composites*, 94:255–263, 2018.

[47] Yu Cheng, Asad Hanif, E. Chen, Guancong Ma, and Zongjin Li. Simulation of a novel capacitive sensor for rebar corrosion detection. *Construction and Building Materials*, 174:613–624, 6 2018.

[48] Austin Downey, Mohammadkazem Sadoughi, Simon Laflamme, and Chao Hu. Fusion of sensor geometry into additive strain fields measured with sensing skin. *Smart Materials and Structures*, 27(7):075033, 2018.

[49] Xiangxiong Kong, Jian Li, William Collins, Caroline Bennett, Simon Laflamme, and Hongki Jo. Sensing distortion-induced fatigue cracks in steel bridges with capacitive skin sensor arrays. *Smart Materials and Structures*, 27(11):115008, 2018.

[50] Théodore Gautier LJ Bikoko, Jean Claude Tchamba, and Felix Ndubisi Okonta. A comprehensive review of failure and collapse of buildings/structures. *International Journal of Civil Engineering and Technology*, 10(3), 2019.

[51] Kumalasari Wardhana, Fabian C Hadipriono, and F Asce. Analysis of recent bridge failures in the united states.

[52] Sdiq Anwar Taher, Jian Li, Jong-Hyun Jeong, Simon Laflamme, Hongki Jo, Caroline Bennett, William N. Collins, and Austin R. J. Downey. Structural health monitoring of fatigue cracks for steel bridges with wireless large-area strain sensors. *Sensors*, 22(14):5076, jul 2022.

[53] Hristiyan Stoyanov, Matthias Kollosche, Denis N McCarthy, and Guggi Kofod. Molecular composites with enhanced energy density for electroactive polymers. *Journal of Materials Chemistry*, 20(35):7558–7564, 2010.

[54] Jan Chan Huang. Carbon black filled conducting polymers and polymer blends. *Advances in Polymer Technology*, 21:299–313, 12 2002.

[55] Austin Downey, Anna Laura Pisello, Elena Fortunati, Claudia Fabiani, Francesca Luzi, Luigi Torre, Filippo Ubertini, and Simon Laflamme. Durability and weatherability of a styrene-ethylene-butylene-styrene (sebs) block copolymer-based sensing skin for civil infrastructure applications. *Sensors and Actuators A: Physical*, 293:269–280, 2019.

[56] Mohammadkazem Sadoughi, Austin Downey, Jin Yan, Chao Hu, and Simon Laflamme. Reconstruction of unidirectional strain maps via iterative signal fusion for mesoscale structures monitored by a sensing skin. *Mechanical Systems and Signal Processing*, 112:401–416, 2018.

[57] Han Liu, Simon Laflamme, Jian Li, Caroline Bennett, William Collins, Austin Downey, Paul Ziehl, and Hongki Jo. Investigation of surface textured sensing skin for fatigue crack localization and quantification. *Smart Materials and Structures*, 30(10):105030, 2021.

[58] Peter Roberts, Dana D Damian, Wanliang Shan, Tong Lu, and Carmel Majidi. Soft-matter capacitive sensor for measuring shear and pressure deformation. In

2013 IEEE International Conference on Robotics and Automation, pages 3529–3534. IEEE, 2013.

[59] Han Liu, Simon Laflamme, Jian Li, Caroline Bennett, William Collins, Austin Downey, and Hongki Jo. Experimental validation of textured sensing skin for fatigue crack monitoring. In *Sensors and Smart Structures Technologies for Civil, Mechanical, and Aerospace Systems 2021*, volume 11591, pages 345–351. SPIE, 2021.

[60] Han Liu, Simon Laflamme, and Matthias Kollosche. Paintable silicone-based corrugated soft elastomeric capacitor for area strain sensing. *Sensors*, 23(13):6146, 2023.

[61] Lingyun Wang, Yu Wang, Su Yang, Xiaoming Tao, Yunlong Zi, and Walid A Daoud. Solvent-free adhesive ionic elastomer for multifunctional stretchable electronics. *Nano Energy*, 91:106611, 2022.

[62] Atsushi Nishino. Capacitors: operating principles, current market and technical trends. *Journal of power sources*, 60(2):137–147, 1996.

[63] B-H Jo, Linda M Van Lerberghe, Kathleen M Motsegood, and David J Beebe. Three-dimensional micro-channel fabrication in polydimethylsiloxane (pdms) elastomer. *Journal of microelectromechanical systems*, 9(1):76–81, 2000.

[64] Fei Feng and Lin Ye. Morphologies and mechanical properties of polylactide/thermoplastic polyurethane elastomer blends. *Journal of Applied Polymer Science*, 119(5):2778–2783, 2011.

Appendix A

IOPScience Copyright for manuscript

This article was published under gold open access model

Copyright and permissions relating to articles published under the gold open access model

For articles published under the gold open access model, in the case of IOP owned journals, the authors retain the copyright in the article and grant IOP a non-exclusive licence to publish it. The position with other journals may vary and is set out in the applicable copyright form.

If an article has been published under the gold open access model, it should have a box with OPEN ACCESS on it at the top of the first page of the article and the licence type at the bottom of the first page of the article.

Most articles published under the gold open access model by IOP are published under a Creative Commons Attribution (CC BY) licence. The CC BY licence allows readers and other users of the article to copy, redistribute, adapt, and build upon the article for any purpose, provided they give appropriate credit to the author(s).

For journals published in partnership with the Electrochemical Society, authors have the choice of publishing under either a CC BY licence or a CC BY-NC-ND licence.

Gold open access articles published prior to December 2012 were published under the CC BY-NC-SA licence.

Appendix B

SPIE Permission to use manuscript

Ogunniyi, Emmanuel

To: Courtney Kendall <courtneyk@spie.org>

Dear Courtney,

I hope this email finds you well. I'm a graduate student in the Mechanical Engineering department at the University of South Carolina, Columbia, and I'm currently preparing my thesis. I'd like to include a paper I authored titled "Soft Elastomeric Capacitors with an Extended Polymer Matrix for Strain Sensing on Concrete," which was published in the 2023 SPIE Smart Structures.
As the primary author of this paper, I'm seeking permission or the appropriate copyright clearance to incorporate it into my thesis. I appreciate your assistance with this matter.

Warm regards,

Emmanuel

Lisa Haley <lisah@spie.org>

To: Courtney Kendall <courtneyk@spie.org>

Cc: Ogunniyi, Emmanuel

Emmanuel hello and good day,

Thank you for your email and questions on how to use your published paper. Since you are an author on the paper you have permission to use it in your thesis. Please make sure though to cite the published parts you use accordingly. If you have any other questions

please let me know.

Sincerely

Lisa M. Haley

Proceedings Coordinator

SPIE – the international society for optics and photonics

lisah@spie.org

Tel: +1 360 685 5603

Fax: +1 360 647 1446

From: Courtney Kendall <courtneyk@spie.org>

Sent: Monday, October 23, 2023 12:56 PM

To: Lisa Haley <lisah@spie.org>

Subject: FW: SPIE paper copyright

Hi Lisa,

Can you answer this author's question? This is for SS23's paper 12486-49.

Thanks,

Courtney

From: Ogunniyi, Emmanuel <OGUNNIYI@email.sc.edu>

Sent: Monday, October 23, 2023 9:25 AM

To: Courtney Kendall <courtneyk@spie.org>

Subject: SPIE paper copyright